# DISSERTATION

On

# A Bond Graph Approach to the Modelling of Cardiovascular System with Embedded Autonomic Nervous System

*Submitted in partial fulfilment of the requirement for the award of degree*

*of*

**Master of Engineering**

IN

**CAD/CAM Engineering**


*Submitted by*

**Kartik Sharma**

**Roll No.: 801481012**

**Under the Supervision of**

**Dr. Tarun Kumar Bera**

*Associate Professor*

*Department of Mechanical Engineering*

*Thapar University, Patiala*



**DEPARTMENT OF MECHANICAL ENGINEERING**

**THAPAR UNIVERSITY**

**PATIALA-147004, INDIA**


**JULY-2016**

# Declaration

I hereby declare that work done in this seminar report entitled, "**A Bond Graph Approach to the Modelling of Cardiovascular System with Embedded Autonomic Nervous System**" submitted towards partial fulfilment of requirement for award of **Master of Engineering degree** in **CAD/CAM Engineering** in **Mechanical Engineering Department** of **Thapar University, Patiala**, is an authentic record of work carried out by me under the supervision and guidance of **Dr. Tarun Kumar Bera, Associate Professor** of **Mechanical Engineering Department, Thapar University, Patiala.**

This matter embodied in this report has not been submitted in part or full to any other university or institute for the award of any degree.

Kartik Sharma

This is to certify that above declaration made by the student concerned is correct to the best of my knowledge and belief.

Tarun Kumar Bera 15/7/16

**Dr. Tarun Kumar Bera**

*Associate Professor*

*Department of Mechanical Engineering*

*Thapar University, Patiala*

**Countersigned by:**

**Head of ME Department,**

**Thapar University, Patiala.**

**Dean of Academic Affairs,**

**Thapar University, Patiala.**

# Acknowledgement

Words often fall short to reveal one's deepest regards. Understanding that a work like this can never be accompanied by the efforts of a single person, I would be obliged to express my profound gratitude and respect to all the people who helped me throughout the duration of this work.

I would like to thank my supervisor, Dr. Tarun Kumar Bera, Associate Professor, Mechanical Engineering Department, Thapar University, Patiala and for his unreserved guidance, constructive suggestions, thought provoking discussions and unabashed inspiration in the nurturing work. They also provided the help in technical writing and presentation style and I found their guidance to be extremely valuable.

I am also thankful to Dr. S. K. Mohapatra, Sr. Professor and Head, Mechanical Engineering Department for providing the facilities for the completion of work.

Finally, I am grateful to my family and friends, without their encouragement, patience and moral support, it would not have been possible for me to complete my thesis.

Kartik Sharma

Reg. No. 801481012

# Abstract

The study of control of cardiovascular system (CVS) by autonomic nervous system (ANS) has been very useful in detection of different types of cardiovascular disorders. The data gathered during different tests of the ANS like Valsalva manoeuvre and tilt test *etc*. are not so easy to analyse, mainly due to the very complex mechanisms involved in the regulation of the CVS. However, model-based analysis of test obtained data has been proposed in a few literature in order to cope with this problem but only a very few models have successfully demonstrated the exact anatomical working of the CVS.

In this thesis, a very basic model of CVS is presented with the dynamics of blood flowing throughout the body. A new model of the ANS, representing the baroreceptors, the sympathetic action and ventricular muscles is also presented. The models have been developed using the bond graph formalism, as it offers a simple and unified representation for all energy domains and facilitates the integration of mechanical, hydraulic and electrical phenomenon. ANS regulation of cardiac contractility is represented by means of continuous transfer functions. The results in terms of cardiac contractility and end systolic pressure (ESP) are presented for two different experiments. Another model is proposed to represent ANS action in terms of an overwhelming controller. Such a controller can also be used in devices like left ventricular assist device.

**Key Words**: Cardiovascular system, autonomic nervous system, blood pressure, baroreflex system, overwhelming controller, bond graph modelling, maximum ventricular elastance, end systolic pressure

# List of acronyms

| | | |
|---|---|---|
| ANS | ≡ | Autonomic nervous system |
| BP | ≡ | Blood pressure |
| BR | ≡ | Baroreflex |
| CVCC | ≡ | Cardiovascular control centre |
| CVS | ≡ | Cardio vascular system |
| ECG | ≡ | Electrocardiogram |
| ESP | ≡ | End systolic pressure(s) |
| MAP | ≡ | Mean arterial pressure |
| NTS | ≡ | Nucleus tractus solitarii |
| PC | ≡ | Pulmonary circulation |
| SC | ≡ | Systemic circulation |
| TMT | ≡ | Treadmill test |

# Nomenclature

| | |
|---|---|
| A | Slope of maximum elastance line |
| $A_c$ | Area of vena contracta |
| $A_o$ | Area of the orifice |
| B | Slope of ventricular filling curve |
| $D_0$ | Denervation level |
| E | Generalized effort |
| $E_{max}$ | Maximum elastance of the left ventricle |
| F | Generalized flow |
| $G_h$ | Gain in hypothalamus |
| $G_n$ | Gain in NTS |
| $I_c$ | Overwhelming controller inertance |
| $I_{P_{ar}}$ | Inertance of pulmonary arteries |
| $I_{P_{AR}}$ | Inertance of pulmonary artery |
| $I_{P_{vn}}$ | Inertance of pulmonary veins |
| $I_{S_{ao}}$ | Inertance of aorta |
| $I_{S_{ar}}$ | Inertance of systemic arteries |
| $I_{S_{vn}}$ | Inertance of systemic veins |
| $K_1$ | Baroreceptor gain |
| $K_2$ | Sympathetic gain |
| $K_c$ | Overwhelming controller compliance |
| $K_{P_{la}}$ | Left atrial Compliance |

| | |
|---|---|
| $K_{P_{AR}}$ | Compliance of pulmonary artery |
| $K_{P_{ar}}$ | Compliance of pulmonary arteries |
| $K_{P_{vn}}$ | Compliance of pulmonary veins |
| $K_{S_{ao}}$ | Compliance of aorta |
| $K_{S_{ar}}$ | Compliance of systemic arteries |
| $K_{S_{ra}}$ | Right atrial compliance |
| $K_{S_{vn}}$ | Compliance of systemic veins |
| $L_1$ | Baseline value |
| $P_{vent}$ | Ventricular pressure |
| $P_u$ | Pressure in first section of orifice |
| $R_{av}$ | Aortic valve resistance |
| $R_c$ | Overwhelming controller resistance |
| $R_{mv}$ | Mitral valve resistance |
| $R_{pv}$ | Pulmonary valve resistance |
| $R_{P_{ar}}$ | Resistance of pulmonary arteries |
| $R_{P_{AR}}$ | Resistance of pulmonary artery |
| $R_{P_{vn}}$ | Resistance of pulmonary veins |
| $R_{S_{ao}}$ | Resistance of aorta |
| $R_{S_{ar}}$ | Resistance of systemic arteries |
| $R_{S_{vn}}$ | Resistance of systemic veins |
| $R_{tv}$ | Tricuspid valve resistance |
| $T_1$ | Baroreceptor time constant |
| $T_2$ | Sympathetic time constant |
| $V_s$ | Stroke volume |

| | |
|---|---|
| $V_u$ | Velocity of first section of orifice |
| $V_{vent}$ | Ventricular volume |
| $\alpha$ | Overwhelming controller gain |

# Subscripts

| | |
|---|---|
| ao | aorta |
| ar | arteries |
| av | Aortic valve |
| AR | Artery |
| c | Overwhelming controller |
| h | hypothalamus |
| la | Left atrium |
| lv | Left ventricle |
| mv | Mitral valve |
| n | NTS |
| pv | Pulmonary valve |
| P | Pulmonary |
| ra | Right atrium |
| rv | Right ventricle |
| S | Systemic |
| tv | Tricuspid valve |
| vent | Ventricle |
| vn | Veins |

# List of Figures

# List of Tables

# Table of contents

# Chapter 1 Introduction

Control theory and controller designing are becoming the most sought out fields not only in industrial research but almost in every aspect of the growing world around us. Being topic of focus in this thesis also, its use in clinical research proves its wide applications. The equipment's used in diagnosis, work on their principles only. Not only in diagnostics but the devices meant to replicate the working of different organs also operate on feedback controller basics. Such devices are needed when an organ stops working and demands external help to retain body's homogenous state. The design of such devices requires a good knowledge of dynamics of physiological systems. A very intuitive approach called bond graph technique has been used in modelling physiological systems because of its easy approach in modelling and simulation of dynamic systems having subsystems from different energy domains.

CVS is such a dynamic system where different subsystems are cardiac contractions (mechanical subsystem), blood circulation (hydraulic subsystem), and transmission of signals throughout a cardiac cycle (electrical subsystem) and so on. The first ever theory describing basis for modern modelling of CVS was Hales Windkessel theory by Otto Frank.

This thesis emphasizes the application of the bond graph method in the modelling and simulation of physiological systems. In our work, first of all a bond graph model of CVS is presented based on segmental description of blood vessels [**1-2**] and pressure curves for systemic circulation (SC) and pulmonary circulation (PC) are simulated and studied in detail with explanations of physiology behind different highlighted features in them. SC is the main circulation system considered during explanations. Similar work has been carried out in this field [**3**]. However, this is only a uni-directional approach as only one channel is considered which starts from ventricles and ends up in systemic or pulmonary sides. With ventricles being the sources of initiations here, study in reverse direction is not possible with such a model.

In order to bring the other part also into the picture, a simple bond graph model for baroreflex (BR) mechanism is also developed in the following section. In this work, pressure measured in the arteries is taken as a source to determine a very important ventricular parameter called maximum elastance ( $E_{\max}$ ). The model is completely inspired by the basic

physiology behind BR mechanism and gives results for ideal cases only. Limitation of this model is that it cannot be used to conduct study in case of a diseased person suffering with cardiovascular disorders. Approximate end systolic pressures (ESP) inside the left ventricle are also calculated and plotted at the end of this section. Modifications and uses of ESP - volume ratio i.e. $E_{\max}$ can be studied from earlier descriptions [**4**] in detail.

An overwhelming controller as developed using bond graph in a work to control plant dynamics [**5**] provides robustness against unknown parameters, un-modelled dynamics and disturbances, *etc*. In the last part, a generalised overwhelming controller is developed as a representation of how blood pressure (BP) is controlled by natural control system also called as ANS. The controller very effectively directs the system to follow experimental BP readings recorded during a TMT fed into the system as desired blood pressures. Work done in thesis can further be modified in future to study effects of change in different variables on ANS for example study of effects of age and gender on autonomic control of BP dynamics [**6**]. Role of the ANS in hypertension [**7**] can also be taken into consideration for future work.

### 1.1 Background and motivation

The study of the ANS effects on CVS has been very useful in indicating risks and in time detection of a variety of cardiovascular diseases. The main problem is that the data gathered during different tests of the ANS like tilt test *etc*. are very difficult to analyse, mainly due to the very complex mechanisms involved in the regulation of the CVS. However, a model-based analysis of test obtained data has been proposed in a few literatures as a way to cope with this problem, only a very few models coupling the main elements involved have been presented in the literature. In this thesis, a new model of the ANS, representing the baroreceptors (sensors), the sympathetic action (response of brain centres to regulate BP) and ventricular muscles ($E_{\max}$) is presented. The models of the ANS have been developed using the bond graph formalism, as it proposes a simple and unified representation for all energy domains, which facilitates the integration of mechanical and hydraulic phenomenon. The short-term ANS regulation of cardiac contractility is represented by means of continuous transfer functions. Their results are presented for two different experiments. The motivation for designing a model to give cardiac contractility variation as an output to change in BP's was to study the impact of BP variation on one of the most important parameter of heart. Another model is proposed to represent ANS action in terms of on overwhelming controller. The motivation behind designing such a controller was applying knowledge of a very special

controller studied during the study of bond graph approach so that a model could be prepared which would give quick simulations. Such a controller can also be used in devices like left ventricular assist device. Such devices are meant for maintaining blood flow throughout the body in patients who have undergone either a heart surgery or a heart attack and their heart walls are not efficient enough to pump blood.

## 1.2 Introduction to cardiac contractility

The most important cardiac parameter that has been the highest point of focus throughout the research reported in this thesis is ventricular cardiac contractility. Action of ventricles can better be shown by a PV diagram [**8**]. Four stages of a cardiac cycle that are ventricular filling (Diastole) i.e. stage 1, constant volume contraction i.e. stage 2, ejection of blood (Systole) i.e. stage 3 and constant volume relaxation i.e. stage 4 are represented on PV curve for left ventricle as shown in Fig. 1.1.

The PV diagram can be well characterised using two curves A and B **[9]**. Curve A is relation between filling pressure (venous pressure) and ventricular volume during stage 1. Curve B is relation between discharging pressure and ventricular volume at the time of closing of aortic valve. The slope of this line is an index of the $E_{\max}$ of the ventricle and is different for the both the ventricles.

During the filling of ventricles, the intra-ventricular pressure is as low as venous pressure and during the iso-volumic contraction (stage 2) ends just above arterial pressure. During the ejection stage, the ventricular pressure is approximately equal to the aortic pressure and also reaches the peak pressure during the same stage. Stroke volume is the difference between stage 2 volume i.e. the maximum volume of blood taken inside by the ventricle and stage 4 volume i.e. the minimum volume of blood left inside the ventricle after complete ejection and is represented in graph as $V_s$ .

The curves for the left and right sides of the heart are quite similar, except for the pressure levels. The pressure in the right ventricle reaches about 25 mmHg at the peak of stage 3, while in the left ventricle the pressure rises up to 120–130 mmHg [**10**].

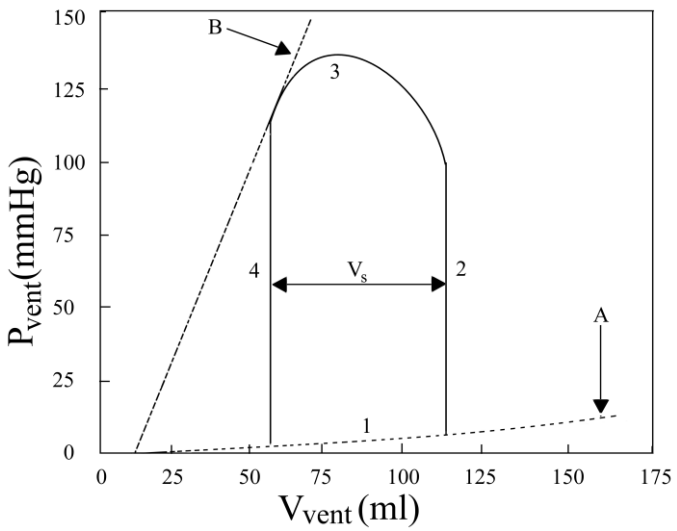


Fig. 1.1 Pressure vs volume diagram for left ventricle

## 1.3 Bond graph approach

Bond graph modelling technique is a technique which utilises the law of conservation of energy to develop a generalised model which is capable of representing systems from different energy-domains. It was developed in 1959, by Prof. H.M. Paynter. The technique works on a model built up by arranging two types of junctions i.e. 1-junction and 0-junction which are further branched and connected with seven types of elements as explained below. These elements represent different plant properties.

### *1.3.1 Introduction to bond graph*

The basic seven elements that are used for representing a system in bond graph technique are I, R, C, Sf, Se, GY and TF. A line segment known as a bond connects all these elements. These bonds represent the flow of power. Flow of power means effort and flow in opposite directions. In one direction effort flows and in the other direction flow flows. Classification of a bond graph model can be done as follows:

- **Single port passive elements**

Inertial element (I), compliance element (C) and resistive element (R) are Single port passive elements. These Single port elements are connected to the system at only one point. These may be active or passive. Active elements are usually sources of power to the system while passive elements only interact with the system power. Single port elements are as explained follows:

**Compliance element**:

The compliance element represented by 'C' is connected to a junction element 1 or 0. It always has an integral causality. It is an energy storage element of the system. It may be graphically as represented in Fig. 1.2.

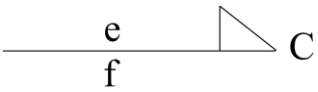


Fig. 1.2 Representation of compliance element

**Inertial element:**

Inertial element represented by 'I' is also an energy storage element. Relationship between effort and flow is given by this I element in such a way that flow can be obtained by integrating effort. It is graphically as represented in Fig. 1.3.

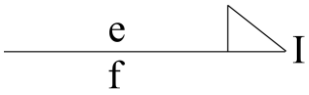


Fig. 1.3 Representation of inertance element

**Resistive element:**

Resistive element represented by 'R', unlike I and C elements which are energy storing elements is an energy dissipater element. R-element may be integrally or differentially causalled depending on the junction it is connected to. It may be graphically represented as shown in Fig. 1.4.

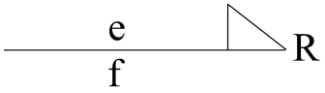


Fig. 1.4 Representation of resistance element

**Source of effort:**

Source of effort represented by 'SE' gives power to the system in the form of effort acting external to the system. Graphically, it may be represented as shown in Fig. 1.5.


Fig. 1.5 Representation of source of effort element

**Source of flow:**

Source of flow represented as 'SF' gives external flow to system. Graphically, it may be represented as shown in Fig. 1.6.


Fig. 1.6 Representation of source of flow element

- **Two port elements**

Two port elements are connected to the system at two points. The two port elements are converters which can convert flow into effort or vice versa or simply multiplies one value to form other depending on the junctions they connect and on the desired values. The 2-port elements in bond graph theory are the 'transformer' and the 'gyrator'. These are represented by 'TF' and gyrator is 'GY', respectively.

**Transformer:**

The transformer neither creates nor destroys energy. It simply redistributes the flow and effort information in between the bond junctions. It magnifies effort from one side to the other and similarly manipulates the flow. The flow multiplication takes place in the direction of arrow and effort multiplication in the opposite. It is as shown in Fig. 1.7.

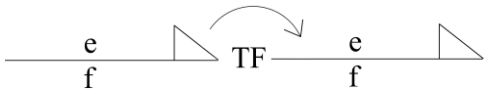


Fig. 1.7 Representation of transformer element

**Gyrator:**

The Gyrator also neither creates nor destroys energy. It simply redistributes the flow and effort information in between the bond junctions. The gyrator element can convert flow into effort and effort into flow. It is usually assigned to a junction representing change in domain. A gyrator element is a s shown in Fig. 1.8.


Fig. 1.8 Representation of gyrator element

- **Junction Elements**

There are two types of junctions, one is 0-junction and the other is 1-junction. These junctions represent a particular state in the system. For example in a mechanical system, 1-junction represents velocity of an object.

**1-Junction:**

1 junction represents flow equality. Suppose power is entering into the junction through bond '1' and leaves through junctions '2' and '3'. Then,

$$p_1 = p_2 + p_3$$

$$e_1 f_1 = e_2 f_2 + e_3 f_3$$

As flows are equal

$$e_1 = e_2 + e_3$$

This means efforts entering and leaving the junction are summed up. Due to this, it is also called as an effort sum junction.

**0-Junction:**

0-junction represents effort equality junction. Suppose power is entering into the junction through bond '1' and leaves through junctions '2' and '3'. Then, $p_1 = p_2 + p_3$ and $e_1 f_1 = e_2 f_2 + e_3 f_3$. As efforts are equal, $f_1 = f_2 + f_3$

This means flows entering and leaving the junction are summed up. Due to this, it is also called as a flow sum junction.

*1.3.2 Bond graph in hydraulics*

Since for modelling a CVS system, knowledge of basics of bond graph for hydraulic systems is very important. Let us consider a hydraulic system as shown in Fig. 1.9.

- **Hydraulic resistance**

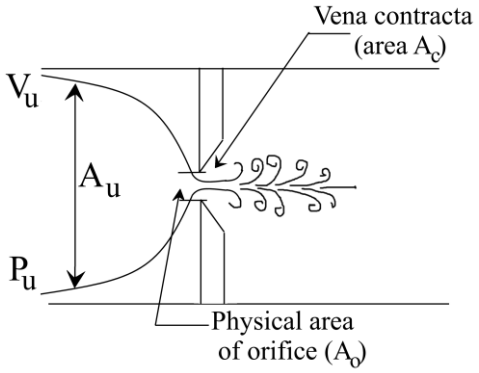


Fig. 1.9 Flow through an orifice

Where,

$A_c$ = Area of vena contracta

$A_o$ = Area of the orifice

$V_u$ = Velocity of first section

$P_u$ = Pressure in first section

So, pressure drop across orifice for the flow of incompressible liquid is given as:

$$\Delta P = \frac{1}{2}\rho\left\{\frac{1}{A_c^{\,2}} - \frac{1}{A_u^{\,2}}\right\}\dot{Q}^{\,2},$$

Or

$$\Delta P = \frac{1}{2}\frac{\rho}{A_c^{\,2}}\left\{1 - \frac{A_c^{\,2}}{A_u^{\,2}}\right\}\dot{Q}^{\,2},$$

Or

$$\dot{Q} = \frac{A_c}{\sqrt{1 - A_c^{\,2}/A_u^{\,2}}}\sqrt{2\Delta P/\rho},$$

Let $A_c = C_c A_o$

Thus,

$$\dot{Q} = \frac{C_c A_o}{\sqrt{1 - (C_c A_c / A_u)^2}}\sqrt{2\Delta P/\rho}$$

Or

$$\dot{Q} = C_d A_o \sqrt{2\Delta P/\rho}$$

where, $C_d = \dfrac{C_c}{\sqrt{1 - (C_c A_c / A_u)^2}}$ = Coefficient of discharge

$$\text{Or} \quad \Delta P = \frac{1}{2}\frac{\rho}{C_d^{\,2} A_o^{\,2}}\dot{Q}^{\,2} = \beta \dot{Q}^{\,2} \tag{1.1}$$

From force equation for dampers we have:

$$F = R\dot{x} \tag{1.2}$$

Comparing Eq. (1.1) and (1.2) we get,

$$R = \beta \dot{Q} \tag{1.3}$$

Equation 1.3 gives resistance for hydraulic systems

- **Fluid Capacitances**

The capacitance reflects storage capacity and is given as the ratio of the volume flow rate and the rate of pressure variation.

Also, $$\Delta P = -\frac{BdV}{V_o}$$

where $V_o$ is the nominal volume of the fluid and $B$ is bulk modulus

So, by definition, $$C = \frac{dp}{dv} = \frac{B}{V_0} \tag{1.4}$$

Equation 1.4 gives compliance for hydraulic systems.

- **Fluid inertance**

It is defined as pressure difference required for unit volume flow rate change.

So, $$dI = \frac{dp(x)}{\dot{q}_v} = \frac{\rho A(x) d(x)\left(\frac{dv(t)}{dt}\right)}{A(x)^2\left(\frac{dv(t)}{dt}\right)} = \frac{\rho x}{A(x)} \tag{1.5}$$

Equation 1.5 gives inertance for hydraulic systems.

### 1.4 Contribution of the thesis

The thesis contributes in following ways:

- Working of CVS is discussed in detail.

- Bond graph model of CVS is presented.
- Simulations of BP in main arteries and arteries are also presented.
- Bond graph model of BR mechanism is also presented.
- Simulation results for $E_{max}$ obtained from this model for experimental blood pressures are also presented.
- Simulation results for ESP in the left ventricle obtained from this model for experimental blood pressures are also presented.
- Bond graph model for ANS is created and discussed in detail with the control mechanism for BP regulation represented by overwhelming controller.
- Simulations obtained from this model showing comparisons for input and output values are also presented.

## 1.5 Organisation of the thesis

This thesis work is divided into 5 chapters which can be summarized as follows:

Chapter 1 introduces the bond graph technique for modelling systems in detail. In addition to this, it also introduces a very important ventricular parameter i.e. cardiac contractility. This chapter concludes with contribution and organisation of the thesis.

Chapter 2 presents literature review done in order to complete this thesis. Its different sections very clearly explains about the literatures surveyed in 3 different fields: CVS, BR and bond graph

Chapter 3 is dedicated to modelling and basics of CVS. First an electrical model of CVS is explained in detail followed by a bond graph model and results obtained from simulations for BP profiles in the body.

Chapter 4 deals with the working and detailed modelling of BR system. Afterwards it shows the variation of $E_{max}$ with BP followed with graphs representing variations of ESP in left ventricle with changes in BP.

Chapter 5 presents conclusions obtained from the research work conducted during thesis work. In addition to this, this chapter also deals with future scopes of the thesis.

# Chapter 2 Literature review

## 2.1 Introduction

This chapter discusses the literature review done for completion of the thesis and the objectives of the thesis. Literature review was done in three areas: (i) Cardiovascular system (CVS) and its working, (ii) Baroreflex (BR) system and its working and (iii) Bond graph modelling technique.

### *2.1.1 Literature survey for CVS*

Cardiovascular engineering is a dedicated field of engineering which deals with studying the dynamics of blood flow in the body. In the clinical world around us, we can see its application from diagnostic devices like electrocardiogram (ECG) and echo to life supporting devices like left ventricular assist devices [**11**]. On the one hand where diagnosis is very important in preventing disease based damages like heart failure and brain strokes *etc.*, on the other hand life supporting devices can give a new life to a patient whose heart has given up on pumping. It senses the BP variation from time to time and does the pumping for heart. It manages proper blood flow and pressure in the body as per the requirement. Such a remarkable discovery for human kind has come into existence just because of advances in cardiovascular engineering.

Cardiovascular engineering is a wonderful combination of physiology, mechanical and electronics engineering. For example, fluid mechanics stream of mechanical engineering plays a role in studying blood mechanics. A research work [**12**] studied the factors influencing flow rate of blood from left atrium to left ventricle. The important outcomes of this research work were pressure difference between the two and rate of ventricular relaxation. A PhD research thesis [**13**] discusses in detail, the mechanical properties of heart and its interaction with the other circulatory parts.

Electronic control theory comes into play in forming control loops similar to the ones responsible for maintaining homeostasis in the body. CVS has also been presented in the form of an electrical circuit [**2**]. The work properly explained the analogies between the electrical and the physiological counterparts of CVS. This paper presented computerised adaptive control of left ventricular assist device for pumping blood in the body. The whole circulatory system was connected with an assist pump with electrical circuits. But the only

part needed for my work is circulatory system which is also presented in Chapter 3 of this thesis. This paper referred a mock circulatory system [**14**] developed in Helmholtz Institute of Biomedical Research, Aachen, Germany as its basic model to develop the electrical circuit and the different parameters were also taken from the same mock model only.

The above mentioned electrical model was worked upon [**2**] to develop a bond graph model for basic circulatory system in human beings. This paper helped us the most in designing the 4 heart valves involved in circulation. It guided the designer to model them as diodes. As the diodes allow only unidirectional flow of current, it is justifiable to model the valves as diodes as the valves also permit blood flow in one direction only because otherwise it might lead to loss of pressure on the other side of the valve due to regurgitation. This paper presented simulation results from Enport 5.2 software. Results included output pressure in PC and SC in addition to pressures in both the atriums and pressures at the valve junctions. This paper was also used to verify my results in Chapter 3.

The bond graph from the above mentioned paper was used [**15**] to conduct simulation based research on studying the role of the ANS in regulation of BP. The simulations were obtained for Valsalva manoeuvre and Tilt test and were compared with the experimental results. The results were obtained for variations in heart rate and BP throughout the tests. The autonomic system connected to the CVS part was taken from a thesis work [**8**] done in association with a Dutch organization for scientific research as PSYCHON project. The mentioned thesis brought into light the other side of BP regulation. It introduced the BR mechanism which served as my second most important area of research after completing my work on forward dynamics of CVS. The next section explains in detail the literature review of the BR system.

### *2.1.2 Literature survey for BR system*

The BR system keeps a check on BP and it regulates various parameters like ventricular elastance, heart rate, venous resistances *etc.*, in case of short term BP regulation and by releasing hormones to involve other organs like kidneys *etc.*, in case of long term BP regulation. A good in depth study of how all these systems coordinate altogether can help us in diagnosis of a problem. A detailed study has been presented in [**8**], which gives knowledge of working of BR mechanism. The main focus of this work has laid upon is short term BP regulation. However, the effects mentioned are in response to mental tasks but the same conclusions can be drawn for a short term physical work out also as both of these tasks

demanded short term BP regulation only. The main 3 parameters this paper took into account to show nervous system response to any kind of task were: maximum ventricular elastance $(E_{\max})$, heart rate and venous resistance. In all these 3 cases, the systems had negative feedbacks which caused the system to alter the changes in BP. However a literature also showed [**16**] that dysfunction of left ventricle during diastole limits the use of maximum $E_{\max}$ as an index of contractile function. The experiment they performed to prove that $E_{\max}$ fails to detect a decline in contractile function when diastolic dysfunction was present included 14 dog hearts. The contractile dysfunction was produced by global ischemia for 60 to 90 minutes followed by reperfusion for 90 minutes. Experiments in literature [**17**] have also been conducted on dogs to study the control of $E_{\max}$ via BR system after and before an artificially induced heart attack. Work has also linked [**18**] $E_{\max}$ to aortic parameters like aortic stroke volume and diastolic and systolic aortic pressures. This literature has given self-explanatory graphs between $E_{\max}$ and the above mentioned aortic parameters separately. This work utilises a very intuitive approach called Buckingham's pie theorem to optimise the relations between all the parameters.

Another work [**19**] picturises very neatly the events that take place on increase in oxygen demand in a particular muscular region during workout. It showed that as the demand increased, the very first response of the system was to increase the heart rate followed by increase in BP. Main emphasis in this study was upon heart rate variation study during a treadmill experiment. The subject ran on treadmill at three different speeds (5, 6 and 7 km/hr). A plot comparing responses of heart rates to all the speeds was also presented in this work. Each time, the readings were taken continuously for around 30 minutes. The running time was divided into 3 parts: resting, exercise and recovery. The plots obtained from the model were compared to these experimentally obtained plots and the error between them was found to be within acceptable range. Conclusively the responses differed for all the three speeds. The responses for 5 and 6 km/hr treadmill experiments were almost similar and attained a steady state very early whereas for the third speed i.e. 7km/hr, it took comparatively more time. Based on the research this paper also proposed a controller controlled treadmill for regulating heart rate during a treadmill exercise. Such a device can play a very important role in designing exercise protocols for athletes and other sportspersons.

An increase or decrease in BP, both are harmful to our body beyond a certain limit. The reviewed literature [**20**] points out that the decrease in BR sensitivity is responsible in many cases for this. BR sensitivity as per the mentioned paper was the increase in pulse interval as a response to rise in systolic pressure. It varied from 1.9 to 48.9 m.sec/mmHg. BR sensitivity differs from person to person and also decreases as the age increases. Another important factor controlling the BR sensitivity is MAP. The study showed that the people who had elevated BP levels in the past but normal pressures at the time of experiments had slightly less sensitivity then the others who didn't have such problems in the past. It also showed the effect of age on sensitivity. According to a research conducted, sensitivity drops down to one third at the age of 60 then what it would have been at an age of 20. Similar kind of work has been reported [**6**] on effect of age and gender on autonomic control of BP dynamics.

From the above mentioned papers I realised that another important factor that I could not afford to neglect in my study was the effect of gender on BR sensitivity. This, I reviewed from a paper [**21**] that discussed about BR differences based on gender and was outcome of an experiment done on 60 patients in anaesthesia condition with their lungs being ventilated mechanically. The outcome of the experiments showed a higher BR gain in males than in females. The effects of age and gender and other studies related to regulation of autonomic system are yet to be included in my modelling and are underscored in my future work perspectives.

### *2.1.3 Literature survey for bond graph modelling technique*

Bond graph technique has become a popular approach since it's initiation in early 1960's for modelling a vast variety of systems. It has found applications not only in conventional engineering fields like mechanical or electrical engineering but also in fields necessitating multi-domain knowledge like biomedical engineering, *etc.* The most highlighting feature of this modelling technique as underscored by many scientists [**22**] across the globe is that it is comparatively very easy for modelling multi-energy subsystems of a very complicated system. The most fascinating feature is that systems need not to be of the same origin. While one subsystem is a mechanical one, other may be hydraulic, electrical or pneumatic one. All these can be merged in a single bond graph connected by power bonds. With these power bonds, flow and effort variables from one system can very easily be converted to the other by manipulations using transformers and gyrators.

The most important literature [**5**] proposed an overwhelming controller for controlling plant dynamics helped me built an alternative bond graph model for representation of role of ANS in BP control. It proposed an overwhelming inversion scheme which controlled a hydraulically driven planar manipulator. The controller was also able to give information about inverse dynamics. For example, for angular inputs on the joints of parallel manipulator, forces could be also calculated. Overwhelming controller is a bond graph based controller which overwhelms the plant properties. This means, doesn't matter what the plant properties are, the system output will always be equal to the desired output.

### 2.2 Literature Gap

It is observed from the extensive literature survey that a lot of work has been carried out in the engineering field on cardiovascular and BR systems. Scientists have shown simulations for BP profiles and also for various ventricular parameters. In fact, the mentioned parameters have been connected to measurable parameters a number of times using a number of techniques. Bond graph modelling technique has also not only been applied successfully on many occasions but has brought revolutionary conclusions also. But this particular section of parameter variation has not been the paragon of focus for bond graph modellers. So, I decided to further extend my initial work of simple cardiovascular dynamics into this direction and model the BR system using the bond graph approach. For the beginning I took $E_{\max}$ as my target parameter and started working on how it could be connected to the BP, we measure using Sphygmomanometer. After the successful modelling of one way BR mechanism whose input was given from the measured BP, modelling a feedback controlled system was a challenge. For modelling a feedback system, overwhelming controller was selected as a controller being from core bond graph background.

### 2.3 Objectives of the Present Work

The beginning of the work as reported in this thesis was an extraction from an already published research conducted on basic CVS dynamics and this model was selected for the initials to set the foundations. The continuation of this work was done in the direction of literature gap mentioned above. So, objectives of this thesis are:

- To present the basics of CVS working for good understanding of basics from physiological plus technical point of view.
- To study the BP profiles along the SC through simulations.
- To study the BP profiles along the PC through simulations.

- To model the BR system as a forward model to give $E_{max}$ (a very important ventricular parameter) as an output to the measured BP. The BP was measured during various workouts (resting, walking and running) and also during a clinical TMT.
- To generate plots for $E_{max}$ inside the left ventricle during the above mentioned experiments.
- To generate plots for ESP inside the left ventricle during the above mentioned experiments.
- To develop an overwhelming controller based feedback controlled system which replicates the ANS controlled human BP regulation system.
- To compare the output and input pressures from overwhelming controller controlled system. The inputs (desired outputs) were pressures fed from TMT readings.

# Chapter 3 The Cardiovascular System

This chapter deals with the detailed explanation of working of CVS, modelling the basics of CVS in terms of electrical analogy and bond graph based modelling. The description and the modelling sections are also accompanied with plots obtained for blood pressures throughout the body. The plots are obtained by simulating the model through Symbols Shakti software.

## 3.1 Introduction to CVS

Cardio-vascular system stands for a remarkable combination of cardiac i.e. heart and vascular (vessels) carrying blood. It is one of the most efficient combinations among the natural systems. Each living organism has this type of system with a wide range of sizes depending on their own development and capacities. Without this system, there would be no life possible among living beings. This system bears the responsibility of transporting nutrients, hormones, oxygen etc. throughout the body. It behaves as an interface between producer and consumer. For example, growth hormones are secreted in the pituitary gland and are carried to other body parts through blood. Another example is insulin which controls blood sugar level in human beings and is pumped to each and every part. Similarly, food is digested in stomach and intestine but the nutrition from food reaches everywhere.

The other important functions CVS are maintaining body BP in a certain range so that enough pressure is there to pump the blood to the very distant parts of the body. In addition, this also prevents veins from getting either too much stretched or too much compressed.

Neural network in our body is dependent on salts for its working. Ions like calcium, sodium and potassium are either taken from food or are generated in kidneys and travel all the way to nervous system for its efficient working. All in all homeostasis is maintained and retained in our bodies only because of proper working of CVS.

CVS is a closed loop structure as shown in Fig. 3.1. Closed loop here means blood is pumped and received back to the heart. Heart acts like a natural pump and serves the purpose of pumping blood. Its own working is fully controlled by the nervous system. Autonomic nervous centre (ANS) continuously works restlessly to control the pumping action of heart without our knowing all this. It controls heart beat and BP day in and day out as per the requirement. No matter we are asleep or awake, resting or running, heart is always under supervision from higher brain centres like hypothalamus etc. A feedback system explained in the later chapter keeps working of heart under control throughout our lifetime. Blood is

pumped from heart into two sides, one is pulmonary and the other is systemic. Pulmonary section disposes off deoxygenated blood in the capillaries surrounding the lungs and takes fresh supply of oxygenated blood from the other side. Systemic compartments carry fresh blood from left ventricle and deliver it to the body parts. This way it nourishes them with nutrition and oxygen and takes back the used up deoxygenated blood back to the heart.

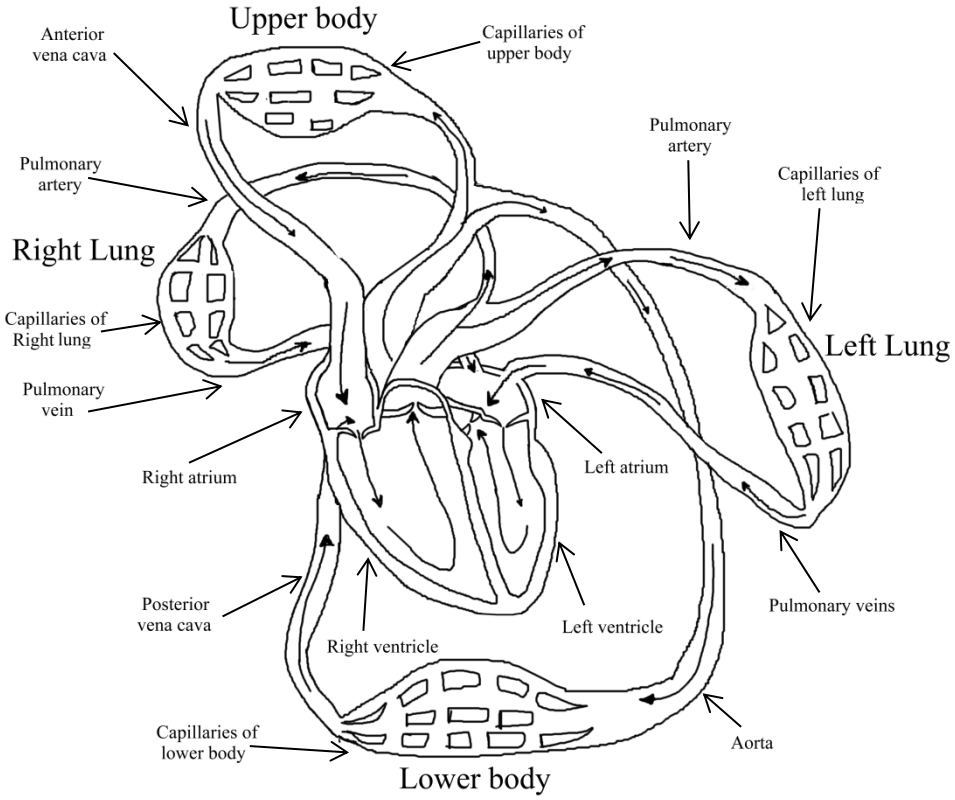


Fig. 3.1 Diagram representation of the CVS

### 3.2 Modelling of CVS

CVS has been modelled as an electrical model representing each component of the system in the form of electrical circuits. The other model discussed in the following section is a bond graph representational model.

*3.2.1 Electrical equivalent model of CVS*

An electrical analogous model [**5**] of the CVS as shown in Fig. 3.2 is used to build a bond graph model. The RLC networks with voltage sources $U_{\text{left}}$ and $U_{\text{right}}$ represents ventricles. $U_{\text{left}}$ and $U_{\text{right}}$ are strengths of the left and right ventricles, respectively. These voltage sources work in the electrical model, the way ventricular muscles work in actual pumping

mechanism of heart for proper circulation of blood throughout the body. The diodes $D_1$ and $D_3$ with resistors $R_{10}$ and $R_5$ collectively model the inlet valves i.e. mitral and tricuspid valves for both the ventricles as shown. Similarly diodes $D_2$ and $D_4$ with resistors $R_1$ and $R_6$ collectively model the outlet valves i.e. aortic and pulmonary valves. Diodes are used to represent unidirectional flow as in case of actual heart valves. Systemic and pulmonary loads are presented by multiple stages of RLC networks. Both $U_{\text{left}}$ and $U_{\text{right}}$ have independent values throughout a cardiac cycle.

Two main parts of the CVS i.e. SC and PC are divided into 3 subparts: Major arteries, arteries and veins. Each subpart is modelled in the same way as a combination of inertance, resistance and capacitance. Each blood vessel is represented by a capacitance in parallel with a series arrangement of resistance and inertia. This arrangement is as explained below.

$R_2$, $L_1$ and $C_2$ form the circuit for aorta with $R_2$ representing the resistance of the aorta, $L_1$ representing the inertia of the aorta and $C_2$ representing the capacitance of the aorta. $R_3$, $L_2$ and $C_3$ form the circuit for systemic arteries with $R_3$ representing the resistance of the systemic arteries, $L_2$ representing the inertia of the systemic arteries and $C_3$ representing the capacitance of the systemic arteries. Similarly, $R_4$, $L_3$ and $C_4$ form the circuit for the systemic veins with $R_4$ representing the resistance of the systemic veins, $L_3$ representing the inertia of the systemic veins and $C_4$ representing the capacitance of the systemic veins. $R_7$, $L_4$ and $C_6$ form the circuit for the pulmonary artery with $R_7$ representing the resistance of the pulmonary artery, $L_4$ representing the inertia of the pulmonary artery and $C_6$ representing the capacitance of the pulmonary artery. $R_8$, $L_5$ and $C_7$ form the circuit for the pulmonary arteries with $R_8$ representing the resistance of the pulmonary arteries, $L_5$ representing the inertia of the pulmonary artery and $C_7$ representing the capacitance of the pulmonary veins. $R_9$, $L_6$ and $C_8$ forms the circuit for the pulmonary arteries with $R_9$ representing the resistance of the pulmonary veins, $L_6$ representing the inertia of the pulmonary veins and $C_8$ representing the capacitance of the pulmonary veins.

Ventricles in the same fashion are represented by a resistance and inertia combination. $R_{Left}$ and $L_{Left}$ represent the resistance and inertance of left ventricle whereas $R_{Right}$ and $L_{Right}$ represent the resistance and inertance of the right ventricle.

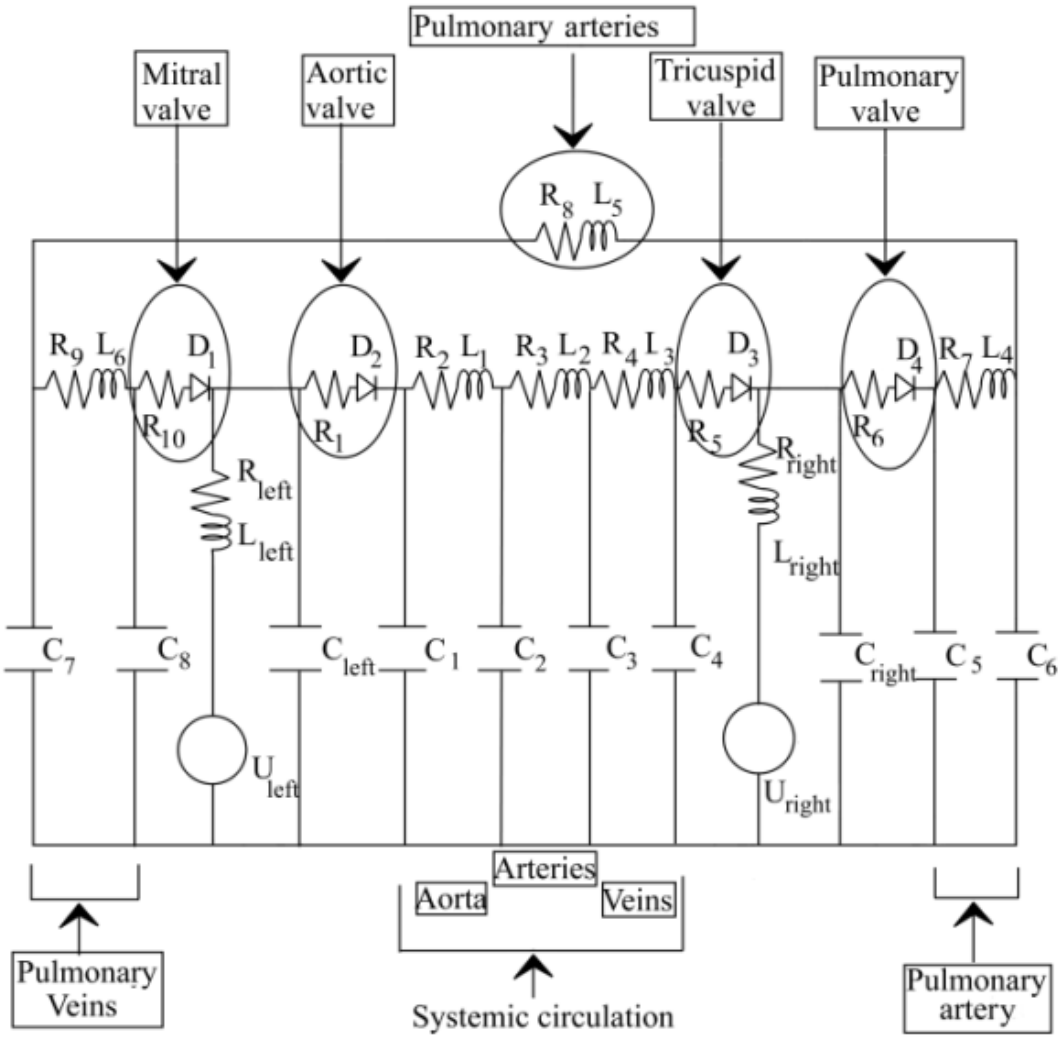


Fig. 3.2: Electrical equivalent model of CVS

*3.2.2 Bond graph model of CVS*

CVS as explained in electrical section consists of two main parts: PC and SC. Bond graph model for both the parts are almost similar as shown in Fig. 3.3. As known, Systemic part deals with blood exchange between all body parts (except lungs) and the heart. It is responsible for delivering oxygenated blood from the heart to all body parts through arteries and carrying deoxygenated blood back from all the body parts to heart through veins. A normal human heart pumps 100,000 times a day and pumps approximately 70 mL blood per beat and 7571 L each day.

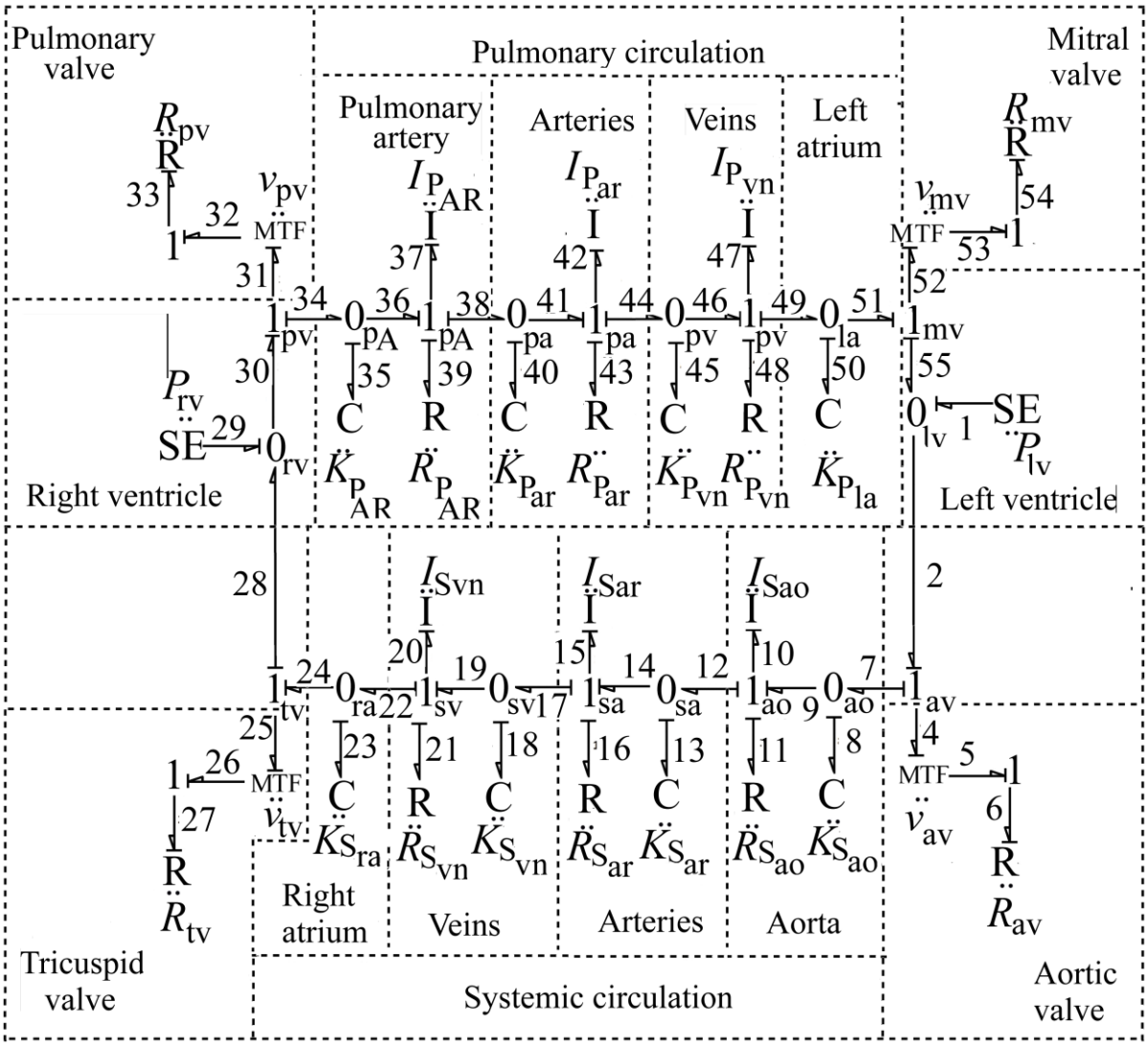


Fig. 3.3 Bond graph model of CVS

Circulation of blood in Systemic part begins with pumping of blood in the left ventricle with $P_{lv}$ representing pressure input to the left ventricle. The corresponding $0_{lv}$ represents pressure in the left ventricle. As from here the oxygenated blood enters into the systemic part of the body via aorta, this 0-junction is followed by junction $1_{av}$ representing volume flow rate between the left ventricle and aorta. This $1_{av}$ junction connects two different 0 pressure junctions to the aortic valve. The aortic valve is modelled as a modulated R-element with modulated transformer value equal to $v_{av}$ and resistance equal to $R_{av}$. $0_{ao}$ represents pressure in aorta, the largest artery carrying blood out from left ventricle. The inertance (I), resistance (R) and capacitance (C) of aorta are represented by $I_{S_{ao}}$, $R_{S_{ao}}$ and $K_{S_{ao}}$, respectively. From aorta the blood enters into systemic arteries with I, R and C represented by $I_{S_{ar}}$, $R_{S_{ar}}$ and $K_{S_{ar}}$.

The $1_{ao}$ junction represents volume flow rate between aorta and systemic arteries. The $0_{sa}$ junction represents pressure in systemic arteries. Blood from arteries is dragged back towards heart through veins carrying blood at a very low pressure. The $1_{sa}$ junction represents volume flow rate between systemic arteries and systemic veins with I, R and C represented by $I_{S_{vn}}$, $R_{S_{vn}}$ and $K_{S_{vn}}$ respectively. The $0_{sv}$ junction represents pressure in systemic veins. The deoxygenated blood from systemic veins enters into the right atrium. The $1_{sv}$ junction represents volume flow rate between systemic veins and the right atrium. The right atrium is represented by a capacitance $K_{S_{ra}}$. The $0_{ra}$ junction represents pressure in the right atrium. From the right atrium blood enters into the right ventricle. The $1_{tv}$ junction represents volume flow rate between the right atrium and the right ventricle. The $1_{tv}$ junction connects two 0-junctions to the tricuspid valve.The tricuspid valve is modelled as a modulated R-element with modulated transformer value equal to $v_{tv}$ and resistance equal to $R_{tv}$.

Blood after entering the right ventricle is pumped into the pulmonary part for bringing fresh oxygenated blood into the system. Modelling of the blood flow in the pulmonary part is same as that of systemic part, beginning with $P_{rv}$ representing pressure input to the right ventricle followed by whole tract including the two valves also modelled in the same fashion as in SC. Fig. 3.4 shows pictorially, how bond graph as explained above can be applied to SC.

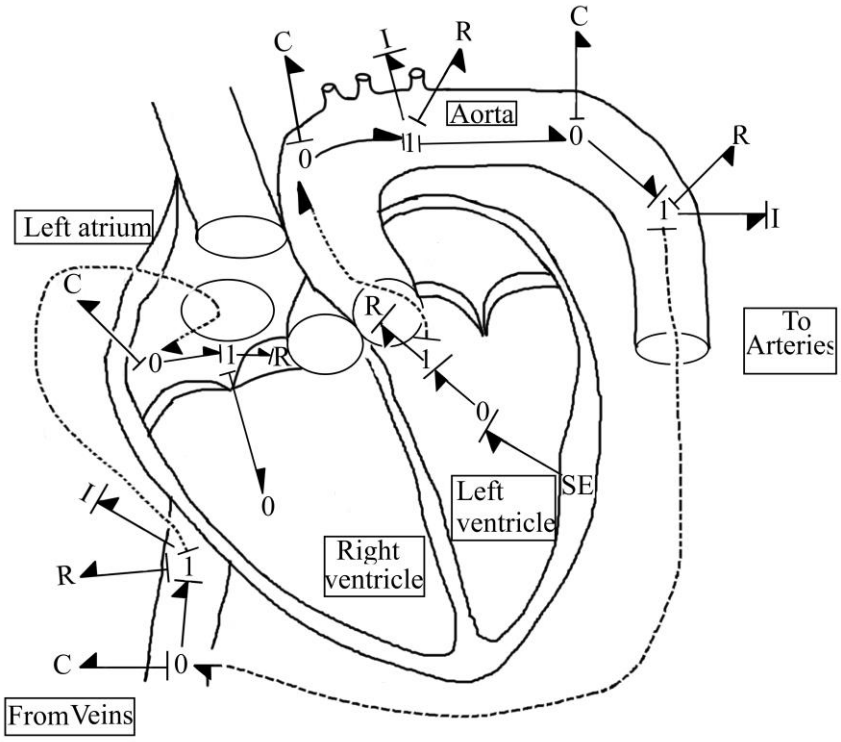


Fig. 3.4 Detailed bond graph model of SC

*3.2.3 Modelling of valves*

Heart valves operate like switches and operate in transitions. Modulated R element [**23**] is used as a solution for modelling this nature of each valve. This modulated transformer element is broken up into a fixed R and a modulated transformer whose modulus $v$ (in general) is a logic variable with values 0 and 1 depending on whether the valve is open or closed, respectively. The modelling of all the 4 valves is done as explained below.

- Aortic valve

Switching of the valves depend upon opening and closing timings. In order to model the aortic valve its modulated transformer values ($v_{av}$) is varied between 0 and 1. Its value is zero in the case when the valve is open. For 0 value of $v_{av}$ no effort is returned into the bond 4 which gives zero effort flow into the direction of $R_{av}$. Zero effort in bond 4 means efforts in bond 2 and 6 are equal. We know that $0_{lv}$ and $0_{ao}$ junctions represent pressure in left ventricle and aorta. So, pressures in both left ventricle and aorta are equal due to no effort (Pressure) loss in between. The BG for this programming is as shown in Fig. 3.5(a).Thus opening of aortic valve is marked with same pressure on both sides.

- Tricuspid valve

In order to model the tricuspid valve its modulated transformer values ($\nu_{\mathrm{tv}}$) is varied between 0 and 1. Its value is zero in the case when the valve is open. For 0 value of $\nu_{\mathrm{tv}}$ no effort is returned into the bond 25 which gives zero effort flow into the direction of $R_{\mathrm{tv}}$. Zero effort in bond 25 means efforts in bond 24 and 28 are equal. We know that $0_{\mathrm{ra}}$ and$0_{\mathrm{rv}}$ junctions represent pressure in right atrium and right ventricle. So, pressures in both right atrium and right ventricle are equal due to no effort (Pressure) loss in between. The BG for this programming is as shown in Fig. 3.5(b).Thus opening of tricuspid valve is marked with same pressure on both sides.

- Pulmonary valve

In order to model the pulmonary valve its modulated transformer values ($\nu_{\mathrm{pv}}$) is varied between 0 and 1. Its value is zero in the case when the valve is open. For 0 value of $\nu_{\mathrm{pv}}$ no effort is returned into the bond 31 which gives zero effort flow into the direction of $R_{\mathrm{pv}}$. Zero effort in bond 31 means efforts in bond 30 and 34 are equal. We know that $0_{\mathrm{ra}}$ and $0_{\mathrm{rv}}$ junctions represent pressure in right atrium and right ventricle. So, pressures in both right atrium and right ventricle are equal due to no effort (Pressure) loss in between. The BG for this programming is as shown in Fig. 3.5(c).Thus opening of tricuspid valve is marked with same pressure on both sides.

- Mitral valve

In order to model the mitral valve its modulated transformer values ($\nu_{\mathrm{mv}}$) is varied between 0 and 1. Its value is zero in the case when the valve is open. For 0 value of $\nu_{\mathrm{mv}}$ no effort is returned into the bond 52 which gives zero effort flow into the direction of $R_{\mathrm{mv}}$. Zero effort in bond 52 means efforts in bond 51 and 55 are equal. We know that $0_{\mathrm{la}}$ and$0_{\mathrm{lv}}$ junctions represent pressure in left atrium and left ventricle. So, pressures in both left atrium and left ventricle are equal due to no effort (Pressure) loss in between. The BG for this programming is as shown in Fig. 3.5(d). Thus opening of Mitral valve is marked with same pressure on both sides.

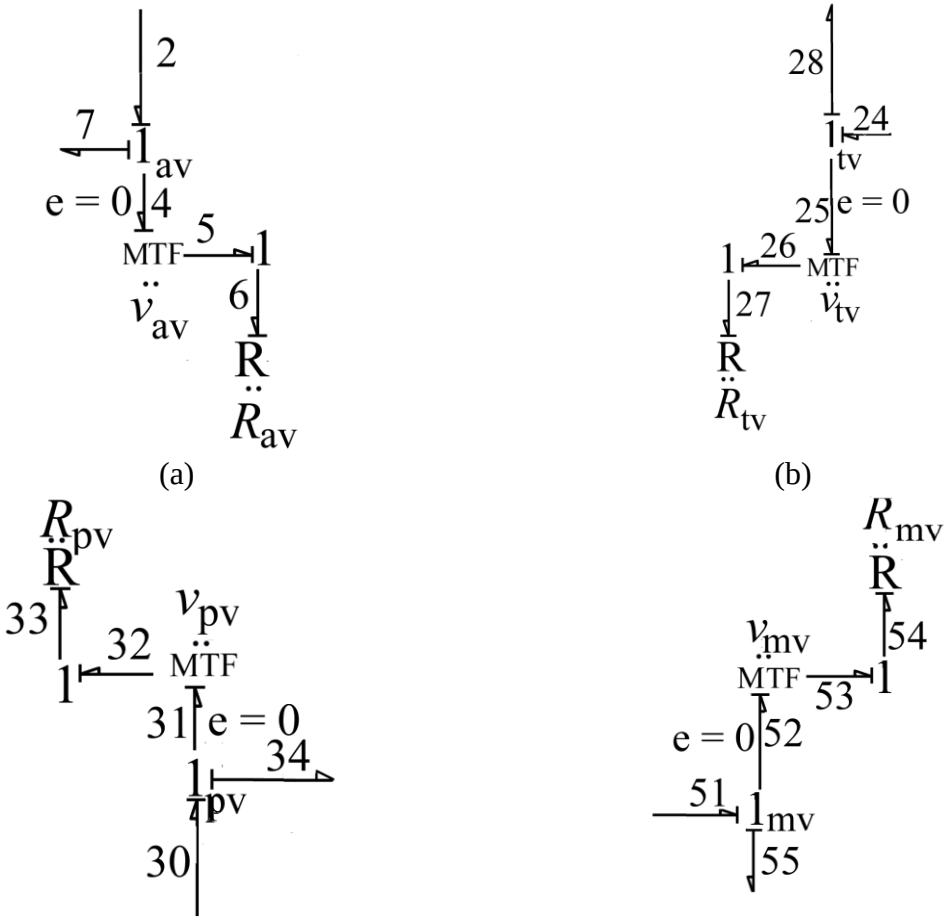


(a) (b) (c) (d)

Fig. 3.5 Detailed bond graph representations of (a) aortic valve, (b) tricuspid valve, (c) pulmonary valve and(d) mitral valve when the valves are open

### 3.3 Parameter values and results

- Parameter values for CVS are given in Table 3.1.

Table 3.1 Parameter values for CVS model

| Parameter name | Value | Source |
|---|---|---|
| Compliance of aorta ( $K_{S_{ao}}$ ) | $6.06\times10^{8}$ N/m$^5$ | [**14**] |
| Resistance of aorta ( $R_{S_{ao}}$ ) | $90\times10^{5}$ Ns/m$^5$ | |
| Inertance of aorta ( $I_{S_{ao}}$ ) | $1.1\times10^{5}$ Ns$^2$/m$^5$ | |
| Compliance of systemic arteries ( $K_{S_{ar}}$ ) | $0.9090\times10^{8}$ N/m$^5$ | |
| Resistance of systemic arteries ( $R_{S_{ar}}$ ) | $1300\times10^{5}$ Ns/m$^5$ | |
| Inertance of systemic arteries ( $I_{S_{ar}}$ ) | $3.1\times10^{5}$ Ns$^2$/m$^5$ | |
| Compliance of systemic veins ( $K_{S_{vn}}$ ) | $1\times10^{7}$ N/m$^5$ | |
| Resistance of systemic veins ( $R_{S_{vn}}$ ) | $25\times10^{5}$ Ns/m$^5$ | |
| Inertance of systemic veins ( $I_{S_{vn}}$ ) | $1.7\times10^{5}$ Ns$^2$/m$^5$ | |

| | | |
|---|---|---|
| Right atrial compliance ( $K_{S_{ra}}$ ) | $2\times10^{7}$ N/m$^5$ | |
| Compliance of pulmonary artery ( $K_{P_{AR}}$ ) | $14.92\times10^{8}$ N/m$^5$ | |
| Resistance of pulmonary artery ( $R_{P_{AR}}$ ) | $45\times10^{5}$ Ns/m$^5$ | |
| Inertance of pulmonary artery ( $I_{P_{AR}}$ ) | $1\times10^{5}$ Ns$^2$/m$^5$ | |
| Compliance of pulmonary arteries ( $K_{P_{ar}}$ ) | $5\times10^{7}$ N/m$^5$ | |
| Resistance of pulmonary arteries ( $R_{P_{ar}}$ ) | $110\times10^{5}$ Ns/m$^5$ | |
| Inertance of pulmonary arteries ( $I_{P_{ar}}$ ) | $2.4\times10^{5}$ Ns$^2$/m$^5$ | |
| Compliance of pulmonary veins ( $K_{P_{vn}}$ ) | $3.33\times10^{6}$ N/m$^5$ | |
| Resistance of pulmonary veins ( $R_{P_{vn}}$ ) | $25\times10^{5}$ Ns/m$^5$ | |
| Inertance of pulmonary veins ( $I_{P_{vn}}$ ) | $1.7\times10^{5}$ Ns$^2$/m$^5$ | |
| Left atrial Compliance ( $K_{P_{la}}$ ) | $2\times10^{7}$ N/m$^5$ | |
| Aortic valve resistance ( $R_{av}$ ) | $1\times10^{13}$ Ns/m$^5$ | Estimated |
| Tricuspid valve resistance ( $R_{tv}$ ) | $1\times10^{13}$ Ns/m$^5$ | |
| Pulmonary valve resistance ( $R_{pv}$ ) | $1\times10^{13}$ Ns/m$^5$ | |
| Mitral valve resistance ( $R_{mv}$ ) | $1\times10^{13}$ Ns/m$^5$ | |

- Results from CVS model

Figure 3.6 presents semi-sinusoidal pressure inputs to the the left and right ventricles. The systolic and diastolic pressure values selected for pressure inputs are similar to the ones mentioned in physiological books and also suggested by physicians. Systolic/diastolic values for left and right ventricular inputs are 120/5 and 21/2 mmHg, respectively. Heart rate is taken constant as 80 beats per minute which means a cycle time of 0.75 seconds for both the ventricles. Valve opening and closing timings [**2**] are given in Table 3.2.

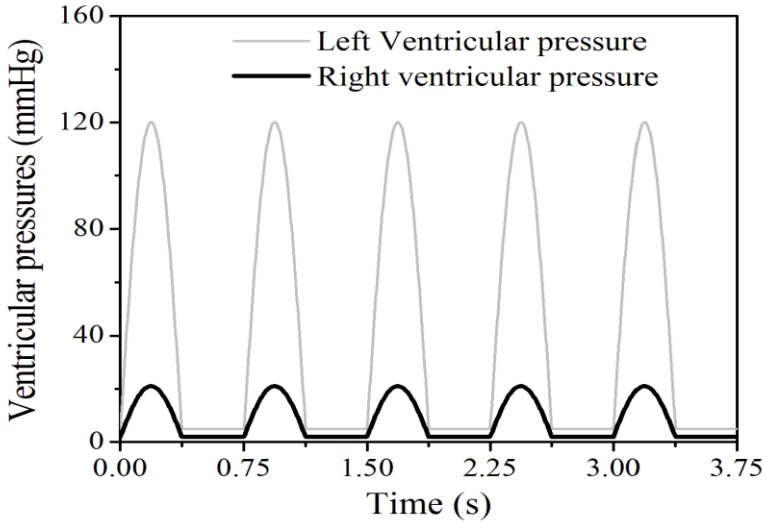


Fig. 3.6 Input pressures to left and right ventricles

Table 3.2 Opening and closing timings for the valves

| Valve | Opening timing (s) | Closing timing (s) | Source |
|---|---|---|---|
| Aortic | 0.077 | 0.250 | [**2**] |
| Tricuspid | 0.361 | 0.001 | |
| Pulmonary | 0.035 | 0.296 | |
| Mitral | 0.374 | 0.001 | |

Figure 3.7 is of important physiological interests. It shows the pressure curves in both SC and PC. As evident from Fig. 3.7, during systole, driving ventricles transmit their complete strength to the major arteries as the valves are open during this period. This can be seen as the same systolic pressures for ventricles and the following major arteries. The same strength is passed on to the systemic and pulmonary arteries but the pressure amplitude decreases as we move further towards the arteries. This is mainly due to the viscous-elastic properties of blood vessels. Another important result that is noticeable is that the diastolic pressure in arteries doesn't fall below a certain limit which is usually around 80 mm Hg in a healthy human being whereas it falls to as low as 5 mm Hg in the ventricle. This can be explained by the fact that after the valve is closed, systemic and pulmonary sides are isolated from ventricular sides and major arteries serve as the second sources of pressure. Another important phenomenon that can be reported in addition to the valve closing for this as a part of interrogation is wave propogation phenomenon. Wave effect is because of forward and backward movement of waves due to multiple reflection sites in vascular system. The

Viscous-elastic properties of vessels are also responsible for the phase lag in presssure wave as it moves down the vascular tree as can be seen from the plots in Fig. 3.7(a). The notch highlighted in Fig. 3.7(a) appears due to valve closing at that time.

It is also evident from Fig. 3.7 that pulmonary compartments have less pressure ranges than their systemic counterparts. Large caliber of pulmonary vessels is responsible for this as they offer lesser resistance to blood flow than systemic compartments.

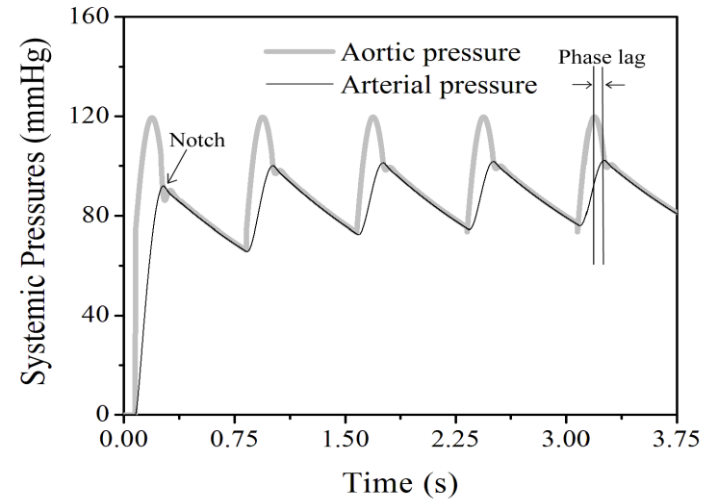


(a)

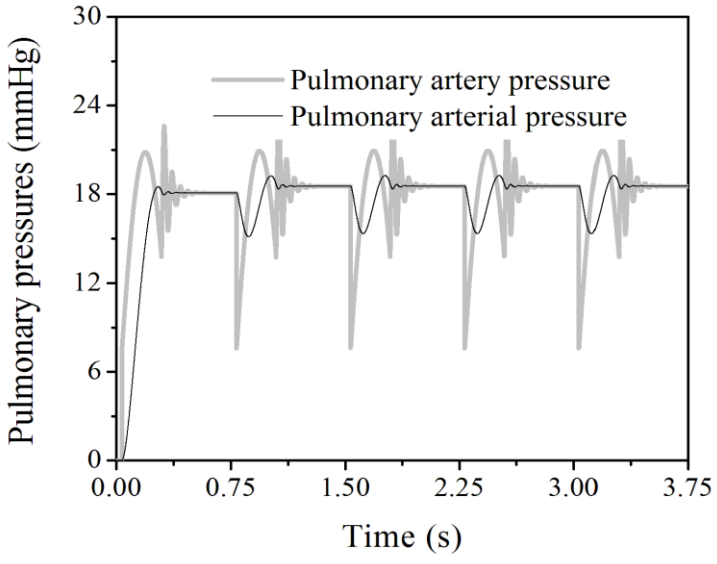


(b)

Fig. 3.7 Output pressures in (a) systemic and (b) pulmonary circulation

# Chapter 4 The Baroreflex System

The work explained in Chapter 3 dealt with only one sided dynamics of CVS as it's initiation began in the ventricles and research could only be done in one direction i.e., in the arterial direction. This limited the scope of work, but my urge to extend my work in the reverse direction led me to study the BR mechanism which works continuously to maintain BP homeostasis in the body. A bond graph model prepared on these basics is also presented in this chapter.

Another model has been developed in this chapter to show the BP regulation mechanism in terms of bond graph. The controller used in representing controller dynamics is bond graph based overwhelming controller.

This chapter has three sections; the first section gives a brief introduction to the working of the BR system. The second section deals with the detailed modelling of all the sub systems involved in its working. It has further 3 sub sections related to each other in the sense that the first one gives us knowledge of engineering behind the working of BR and the rest two apply the knowledge in developing bond graph models in two different ways. The third section has result plots obtained from Symbols Shakti software. Simulations are obtained for inputs from different experiments like BP recordings during resting, walking and running in addition to readings taken during standard TMT from a hospital.

### 4.1 Introduction to BR mechanism

BR mechanism model represents the control mechanism responsible for bringing the BP back to the BR point. The mechanism increases mean arterial pressure (MAP) if it has fallen down from the standard limit and decreases it in case of elevated levels. Thus BR mechanism is a negative feedback mechanism. Controller output which in this case is output from cardiac control centre or controlled input to the heart is used to give a plot of maximum elastance ( $E_{max}$ ) of left ventricular cardiac muscles. The main aim of this work is to plot $E_{max}$ in left ventricle corresponding to normal MAP and for changes in MAP. BR consists of 3 main sections that are baroreceptors, cardiovascularcontrol centre (CVCC) and efferent nerves.

The first participants of control mechanism are sensors which are specialised neurons known as baroreceptors. Baroreceptors are located at different sites throughout the vascular system and are found in the walls of blood vessels but the most important baroreceptors that play role in short term BP control are the ones located in the carotid arteries in the neck

region. This work focusses on carotid baroreceptors mainly. Baroreceptors continuously fires action potentials. An action potential is a short lasting event in which the electrical membrane potential of a cell rapidly rises and falls. Action potentials in neurons are also known as nerve impulses or spikes. A sequence of action potentials generated by neurons is called its *spike train*. Movement of action potential between cells is as shown in Fig. 4.1.

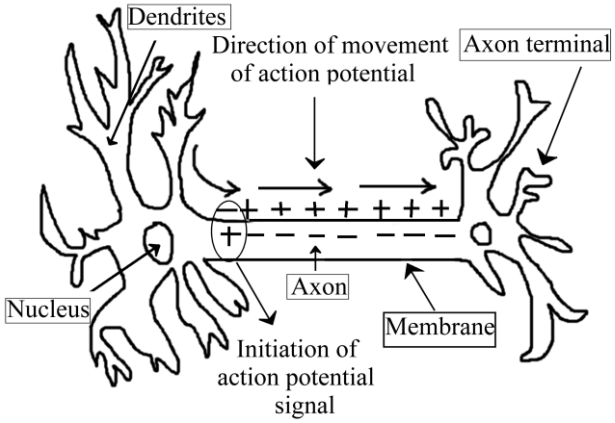


Fig. 4.1 Movement of action potential in nervous system cells

Action potentials are generated by voltage-gated ion channels which are dedicated gates embedded in cell's plasma membrane. These gates are closed when the cell is at resting potential and opens up when the membrane potential increase to a threshold value. Opening and closing of gates is controlled by depolarisation. Depolarisation refers to a sudden change in cell's internal electrical environment and voltage vs time plot is shown in Fig. 4.2. The cells usually maintain an environment that is negative as compared to its surroundings. Thus there is some difference in potential on the two sides called membrane potential. Depolarisation leads to positive charge inside the cell for a very short time. Due to depolarisation there is a change in charges on both sides of the membrane. This shift from negative to positive and vice versa is responsible for the transmission of electrical impulses. This phenomenon is responsible for communication between cells and conducts messages between brain and rest body.

The process of depolarisation depends upon intrinsic electrical nature of cells. When a cell is at rest, it has a resting potential. This condition exists nearly in all cells and during it, they have negative charge inside. This electrical imbalance is maintained inside by positively and negatively charged ions transported across the cell's plasma membrane. The transport of ions across the plasma membrane takes place through different types of transmembrane proteins embedded in the cell's plasma membrane functioning as pathways for ions into and out of the

cells. Resting potential is must for the cell before it can be depolarised. The cell uses ion pumps, ion channels and voltage gated ion channels to generate a negative resting potential. However, an atmosphere outside the cell for depolarisation is also created during the generation of resting potential. The pump mainly responsible for the optimisation of conditions on both sides of membrane for depolarisation is sodium potassium pump. Three positively charged sodium ions ($Na^+$) are pumped out of the cell and two positively charged potassium ions ($K^+$) are pumped into the cell. Thus, concentration of $Na^+$ increases outside the cell and $K^+$ increases inside the cell. Despite the presence of $K^+$ ions, cells contain internal components (negative charge), which accumulates to establish negative inner charge.

Now, as the cell has achieved a resting potential, the cell has attained a capacity to undergo depolarisation. The voltage gated ion channels open up by an electrical stimulus and $Na^+$ ions start moving inside through them. This in turn increases the positive charge inside and cell reaches depolarisation stage.

This phenomenon is followed by repolarisation. In repolarisation, the closed potassium gates open up and $K^+$ ions start moving outside the cell. The process continues until enough negative charge is accumulated inside the cell. Repolarisation is followed by hyperpolarisation. Since during repolarisation, the cell's internal potential falls to a more negative value then what it should have during resting potential, all the gates get closed until the time enough negative charge is accumulated inside the cell to corresponding to resting potential. This whole phenomenon is represented as a graph in Fig. 4.2.

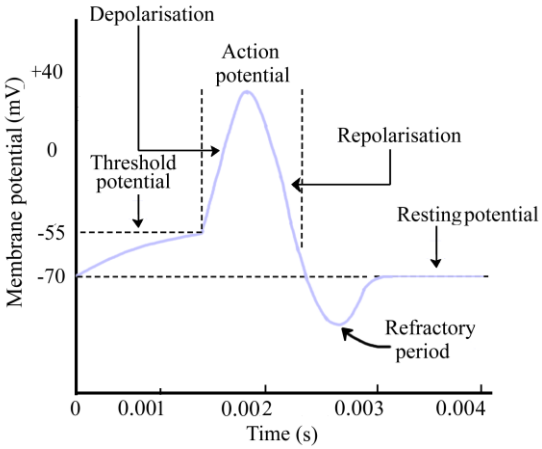


Fig. 4.2 Action potential in a neuron

## 4.2 Modelling of BR system

The basics of BR mechanism are presented in technical form. First, BR is divided into 3 parts and explained in detail with the help of block diagrams. In the second part, a bond graph representational model of BR mechanism is shown. In the third part a model which replaces ANS with a bond graph based overwhelming controller is presented.

### *4.2.1 Physiological model of BR system*

Figure 4.3 showcases the transmissions in the BR mechanism. The BR is the fastest mechanism to regulate even every minute changes in BP by controlling various parameters like heart rate, cotractility and peripheral resistance. The mechanism begins with sensors located in aortic arch and carotid sinus in neck region. Baroreceptors are mechanoreceptors and are responsible for sensing BP changes. They respond to change in tension on the arterial wall [**24-26**] due to change in BP. Impulses from baroreceptors are relayed to nucleus of the tractus solitarius (NTS) which also recieves inputs from higher brain centres like hypothalamus etc. Ultimately the relays reach vasomotor centre which on its part controls sympathetic and parasympathetic drives. The impulse rate keeps on varying throughout the heart cycle [**24-26**] but the mean impulse rate depends mainly on the mean arterial BP [**26-27**].

Sympathetic nervous system nicknamed as *fight or flight response* as we know is that part of nervous system which raises activity level of the heart whereas parasympathetic system on the other hand nicknamed as 'rest and digest system' slows down activity level of the heart. Due to a sudden rise in BP, stretch in baroreceptors causes an increased firing rate.

The impulse rate keeps on varying throughout the heart cycle (**24-26**) but the mean impulse rate depends mainly on the mean arterial BP [**26-28**]. The relation between MAP and firing rate is given by an S curve [**24**] as shown in Fig. 4.4(a). The slope of the curve gives baroreceptor sensitivity. Note from Fig. 4.4(a) that the baroreceptors are most sensitive in normal MAP zone i.e., around 100 mmHg. Baroreceptors become saturated after about 180 mmHg [**28-29**] and are not responsive to MAP below about 40 to 50 mmHg approximately [**25-26**]. When baroreceptors are stimulated by an increased pressure, impulse rate increases suddenly. As a response vasomotor inhibits sympathetic drive and increases parasympathetic drive onthe SA node of the heart. This lowers down heart rate and relaxes the heart by reducing contactility of heart walls. On the other hand, a drop in firing rate is responded by uninhibiting of sympathetic activity and decrease in parasympathetic influence on the heart.

However, if BP remains at an elevated level for more than one day, BR system sets itself to the new BR point. So, the importance of study of BR mechanism is for short term BP regulation only.

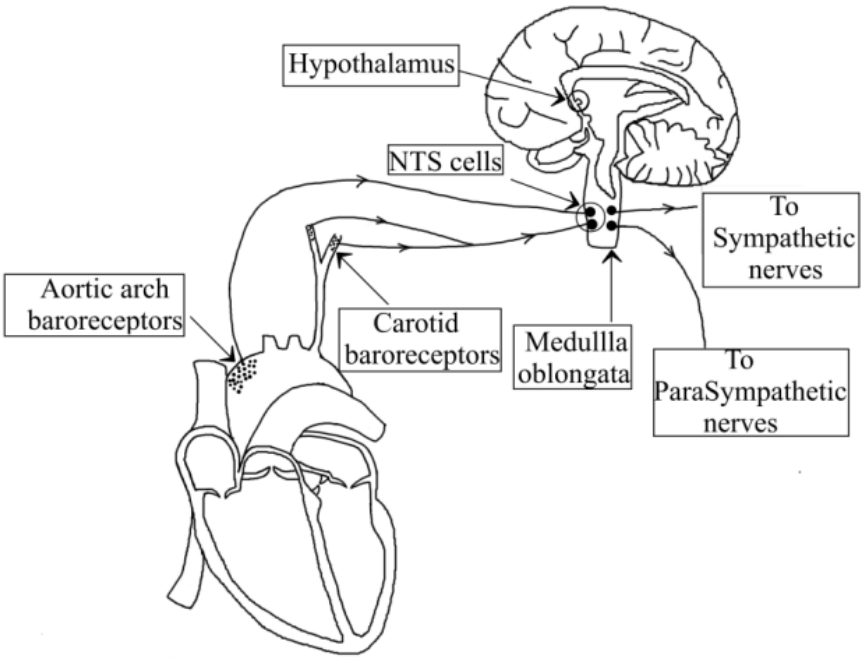


Fig. 4.3 Physiological representation of BR system

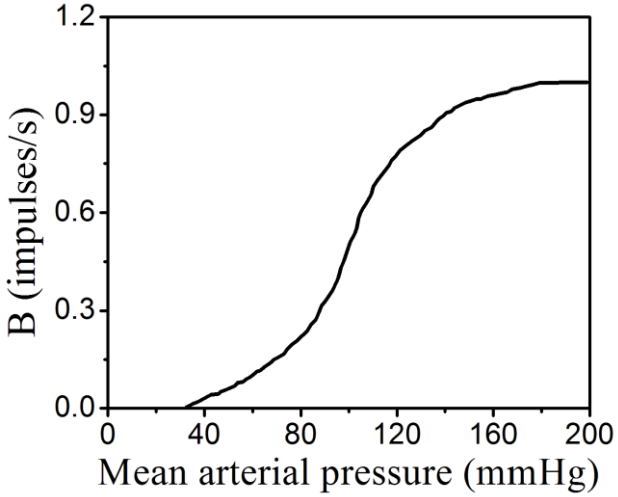


(a)

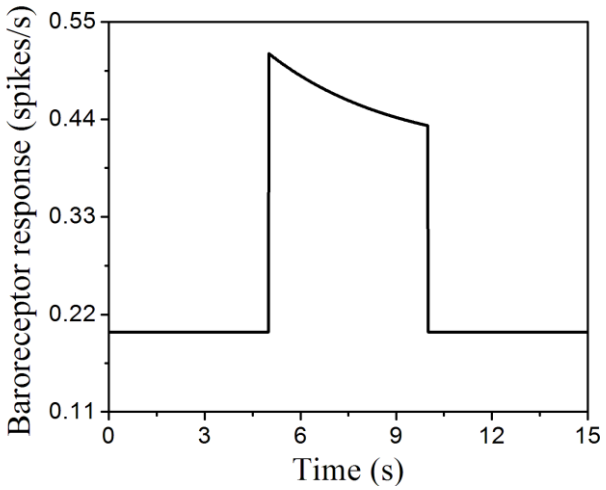

(b)

Fig. 4.4(a) sensitivity curve and (b) response of baroreceptors

Figure 4.5 is a block diagram representation [**8**] of BR mechanism divided into 3 stages as explained in the following sub-sections:

- The Baroreceptors

First stage shown in Fig. 4.5(a) presents baroreceptor activity. MAP, $P_{sa}$ is transformed into relative baroreceptor activity, 'B' and as explained above in detail, this follows an S curve as shown in Fig. 4.4(a).

The dynamic properties of the receptors are modelled as first order system as shown in Fig. 4.5(a). A gain ($K_1$) added in parallel to this first order system, shows the relation between the final baroreceptor output $B_b$ and input B'. The first order system reduces the initial effect ($B_b = K_1 \times B'$) in $T_1$ with the time constant $T_1$. In steady state the response will be ($K_1$-1)× B'. The value of $K_1$ is taken as 2, so, $B_b$ =B' is in the steady state. The response of baroreceptor activity after a pressure step from approximately 78 to 95 mmHg is as shown in Fig. 4.4(b).

- The cardiovascular control centre (CVCC)

The CVCC links baroreceptor output to effector input. It is located in the medulla oblongata and it consists of complex neural structures that integrate baroreceptor inputs. The defence reaction, evoked by external loads like physical tasks or mental tasks etc. begins in the hypothalamus. From the hypothalamus, the activation travels to the CVCC through neural

networks, then to the parasympathetic (vagal) and sympathetic nervous system, and finally to the heart and the blood vessels.

The basic structure of the CVCC is shown in the form of block diagram in Fig. 4.5(b). Baroreceptor activation $B_b$ enters the NTS [**29-31**] and is modulated in a random way by higher brain centres in form of a gain $G_h$ [**31-33**]. Another modulation from the NTS in terms of a gain $G_n$ is involved before the final NTS outcome. But as the role of hypothalamus and NTS in baro-modulation is very uncertain so for simplicity the values for both the gains are taken as 1.

The NTS is innervated not only by neurons from the hypothalamic defence area, but also from nerves coming from higher structures such as the frontal cortex, and amygdala. The medullary structures receiving inputs from hypothalamus are the vagal motor centre and the origin of sympathetic and vagal nerves.

- Maximum Ventricular elastance ( $E_{max}$ ) effector

Figure 4.5(c) depicts $E_{max}$ effector in form of block diagrams. The elastance is controlled by the sympathetic system [**34**]. $D_0$ is denervation level and $L_1$ is baseline value for ventricular elastance.

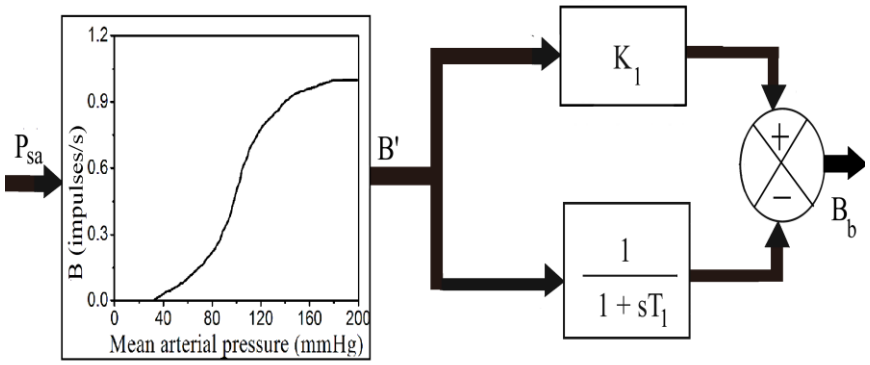


(a)

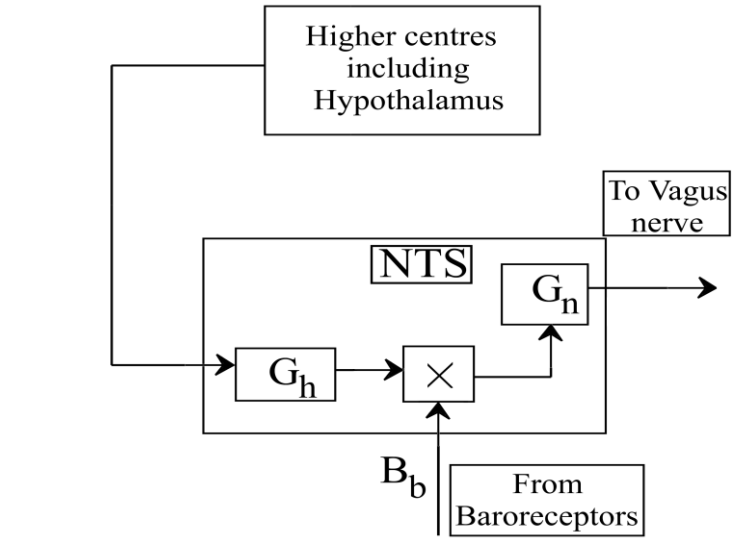


(b)

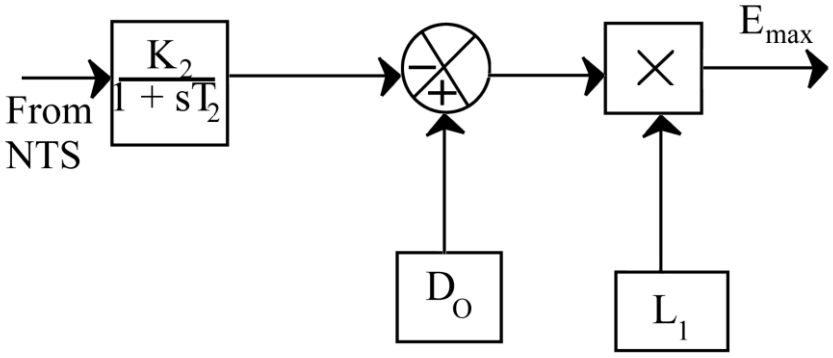


(c)

Fig. 4.5 Block diagrams for (a) Baroreceptor model with first order system in laplace notation, (b) model of cardiovascular control centre and (c) model of the maximum ventricular elastance effector

*4.2.2 Bond graph model for BR mechanism*

Bond graph model of BR is built on the basic models explained in parts in above sections and is shown in Fig. 4.6. It begins with a source of effort input as a step function in terms of baroreceptor activity B relative to MAP from S curve. Three transformer with magnitudes $u_1$, $u_2, u_3$ and represents 3 parts of BR. $u_1$ represents transfer function between input B and output $B_b$ of 1st part; $u_2$ represents a multiple of $G_h$ and $G_n$ i.e., transfer function between $B_b$ and NTS output and $u_3$ represents the transfer function in sympathetic system. Transformer with modulus $u_4$ multiplies sympathetic output at end effector with baseline value for left ventricular elastance. Final outcome of the bond graph, $E_{max}$ for the left

ventricle is obtained as a response for given MAP and is picked up from an effort pickup sensor.

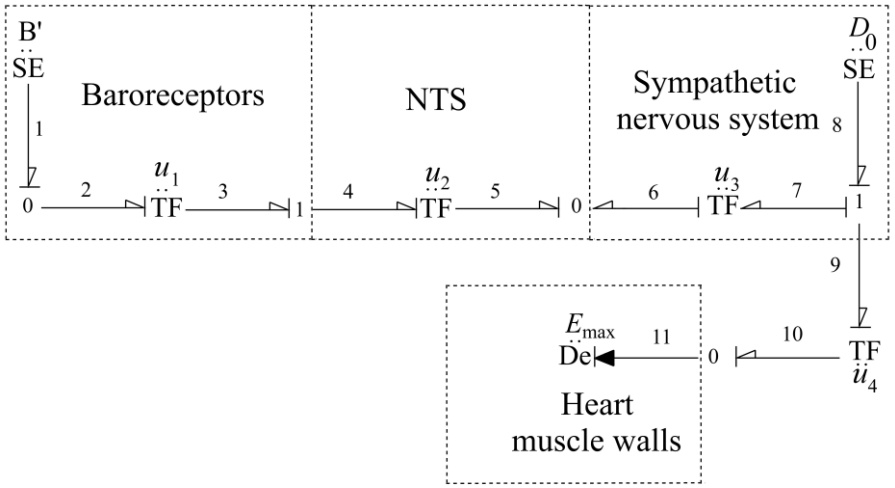


Fig. 4.6 Bond graph for BR mechanism

*4.2.3 Alternative model for BR system using overwhelming controller in place of ANS*

- Modelling of the controller

ANS action in BP control can also be explained by a robust overwhelming controller. The basic concept of overwhelming controller taken into view is that it overwhelms plant properties. The whole plant and controller dynamics are in terms of pressure only as per the requirements.

The error between the reference pressure ( $P_{ref}$ ) and the pressure picked up from arteries ( $P_{sa}$ ) by an effort pick up sensor is applied to a controller through a virtual pressure actuator. The reactive pressure developed by the controller is sensed by a virtual effort sensor (here, virtual sensing means computation). The reactive pressure from controller is scaled through an amplifier gain $\alpha$ and then applied to the plant (SC in specific) in the left ventricle through an effort actuator. The combined causalled bond graph of plant and controller is shown in Fig. 4.7. The transfer-function between $P_{sa}$ and $P_{ref}$ can be obtained from Fig. 4.7 by application of Mason's gain rule.

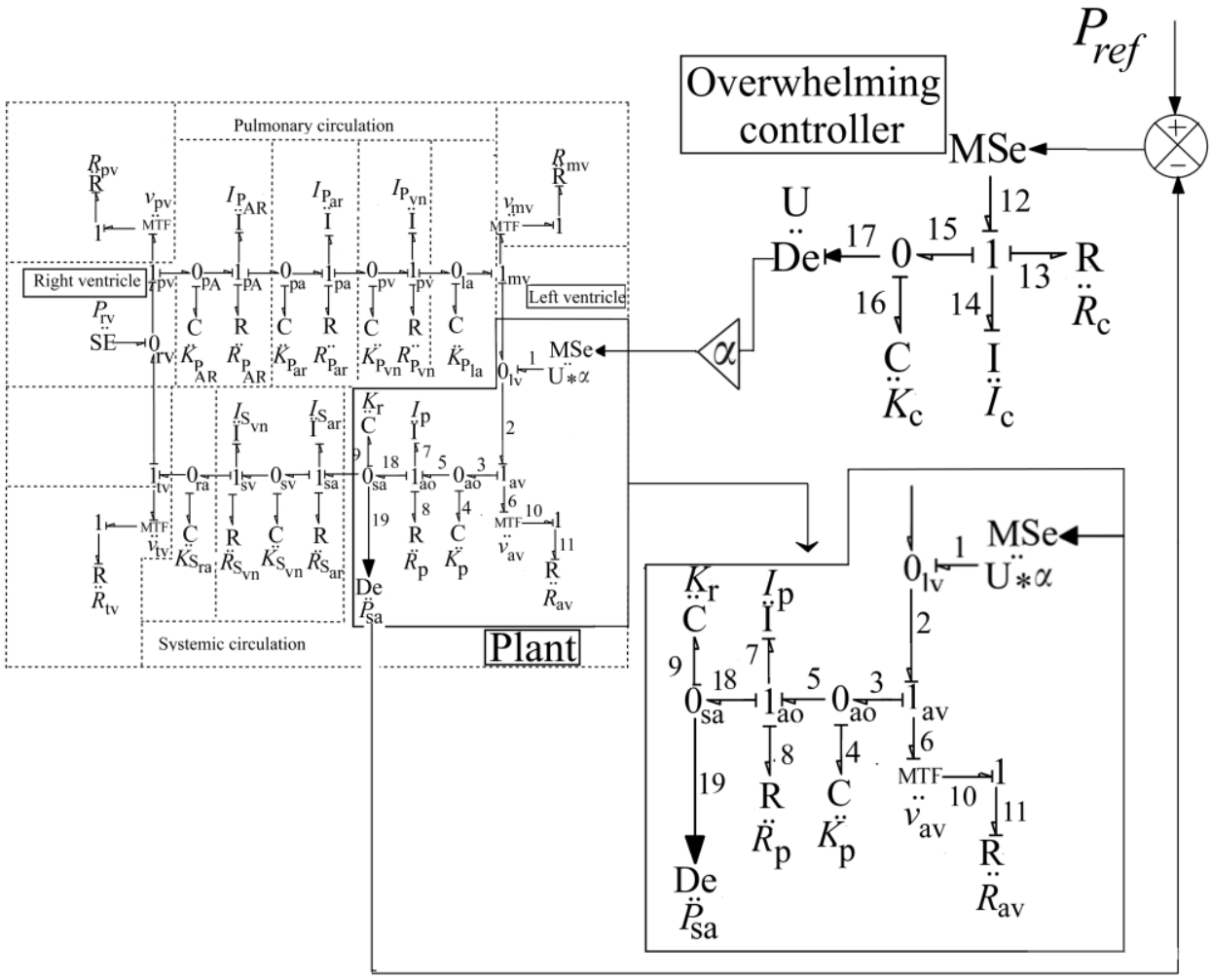


Fig. 4.7 Bond graph model of CVS system with overwhelming controller

$$G(s) = \frac{e_9(s)}{P_{\text{ref}}} = \frac{T_2(s)\alpha}{T_1(s) + T_2(s)\alpha} \tag{4.1}$$

$$T_1(s) = (I_p I_c\, s^4 + I_p R_c\, s^3 + I_c R_p\, s^3 + I_p K_c\, s^2 + I_c K_p\, s^2 + I_c K_r\, s^2 + R_p R_c\, s^2 + K_p R_c\, s + K_r R_c\, s + R_p K_c\, s + K_p K_c + K_r K_c)$$

$$T_2(s) = (K_r K_c)$$

This implies that the plant which is ventricle plus systemic part of CVS here up to arteries, follows the command for pressure if the amplifier gain ( $\alpha$ ) is sufficiently large. $P_{sa}$ follows the same pressure as $P_{\text{ref}}$ . $P_{\text{ref}}$ can be considered as BR set point which system tries to keep arterial pressure at. Now conclusively, if approximately the same pressure values exist for both of them, controller is working well. Further, one may note that the plant parameters ( $I_p$ ,

$R_p$ and $K_p$) appear only in $T_1$(s) and are all overwhelmed by the controller as these plant parameters do not appear in $T_2$(s). However, $K_r$ from plant appears in $T_2$(s) but a combination of $K_c$ and $\alpha$ can still be used to overwhelm the plant properties. Very high values of gain parameter $\alpha$ cannot be taken as a very high gain value may lead to an increase in noise sensitivity and the time required for simulation also increases. Moreover, large gain values may also increase overshoot in the response which may exceed the actuator capacity, i.e.,. may cause actuator saturation. Note from parameter values that controller stiffness ($K_c$) value is also very large. For a large value of $K_c$, G(s) approaches unity even for smaller values of the $\alpha$ and for small value of $K_c$, a large $\alpha$ is required. Therefore, the gain parameter value is designed along with the controller parameter values ($I_c$, $K_c$, and $R_c$). Values for all controller parameters are given in Table 4.1. Parameters for plant are taken same as taken in CVS section. A highlighted view of the concerned part of plant is also shown in right lower corner in Fig. 4.7.

### 4.3 Parameter values and results

*4.3.1 Parameter values and results for BR model*

- Parameter values for BR system are given in Table 4.1

Table 4.1 Parameter values for BR system

| Parameter name | Value | Source |
|---|---|---|
| Baroreceptor gain ($K_1$) | 2 | [**35**] |
| Baroreceptor time constant ($T_1$) | 4 s | |
| Hypothalamus gain ($G_h$) | 1 | Estimated |
| NTS gain ($G_n$) | 1 | |
| Sympathetic gain ($K_2$) | 0.48 | [**36**] |
| Sympathetic time constant ($T_2$) | 10 s | |
| Denervation level ($D_0$) | 1.24 | [**14**] |
| Baseline value ($L_1$) | 1.69 mmHg/cm$^3$ | |

- Results from BR model for experimental BP values

Figures 4.8(a) and 4.8(b) present systolic and diastolic pressures of a subject during resting, walking and running. Both the systolic and diastolic limits of the subject in all the three cases

are almost same initially but the difference grows as time increases. During resting, systolic pressure has a range of 13 mmHg with least and most values being 106 and 119 mmHg respectively while diastolic pressure has a narrow range of 7 mmHg with least and most values being 67 and 74 mmHg respectively. During walking, systolic pressure has a range of 5 mmHg which is less as compared to that during resting but with the least and most values being higher than resting at 117 and 123 mmHg while diastolic pressure has almost the same range of 8 mmHg but with least and most values of 72 and 81 mmHg being higher than resting. During running, the plots for both systolic and diastolic pressures shoot up with time with a broad range in both the values. Systolic pressure has a range of 24 mmHg with least and most values being 118 and 142 mmHg respectively and diastolic pressure has a range of 23 mmHg with least and most values being 73 and 96 mmHg, respectively.

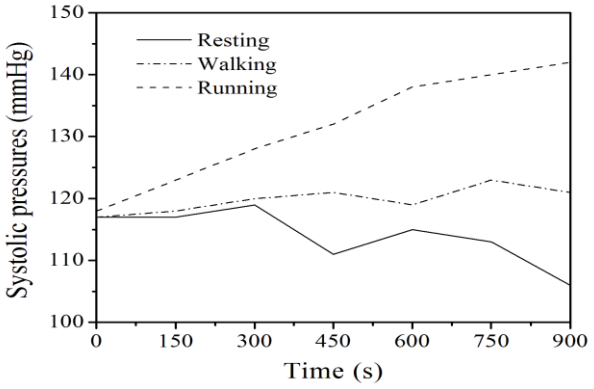


(a)

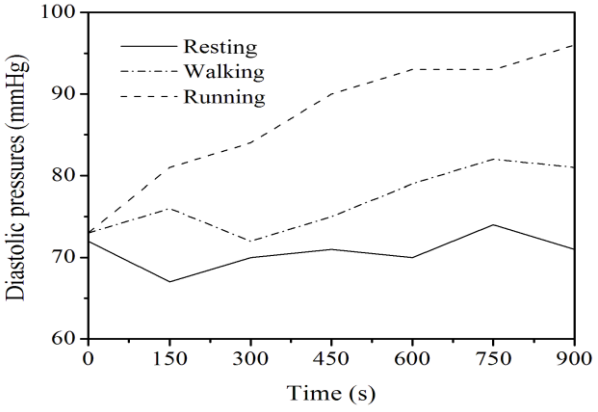


(b)

Fig. 4.8 Experimental (a) systolic and (b) diastolic arterial blood pressures measured during resting, walking and running

Figure 4.9 are plots obtained for maximum elastance ($E_{max}$) of left ventricle from BR model simulations. We know $E_{max}$ represents contractility of heart and also that $E_{max}$ decreases with the increase in MAP and vice versa due to continuous modulations from NTS

and higher brain centres to counteract the changes in MAP from baseline values. This happpens so that heart muscles could relax to bring MAP down for an increase in MAP and could contract with more force to bring MAP up in case it has fallen down from the desired limits. As evident from the graph plots in Fig. 4.9, $E_{max}$ values are changing continuously with change in input values of MAP. There is not much variation in $E_{max}$ for resting with minimum and maximum values of 1.980 and 1.998 mmHg/cm$^3$, respectively. On the other hand, during walking a little more variation is there as compared to resting with minimum and maximum values of 1.926 and 1.972 mmHg/cm$^3$, respectively. During running, lot of variations can be seen with minimum and maximum values of 1.810 and 1.929 mmHg/cm$^3$, respectively. As during running the MAP keeps on increasing with time, the $E_{max}$ value keeps on decreasing with minimum value of 1.810 mmHg/cm3 for MAP of 120 mmHg for systolic/diastolic limits of 160/100 at the end.

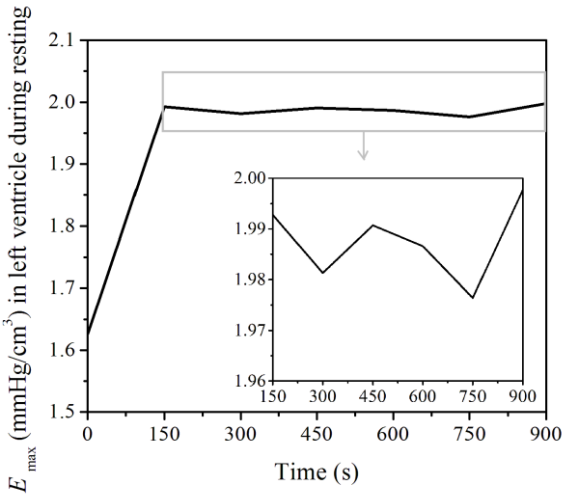


(a)

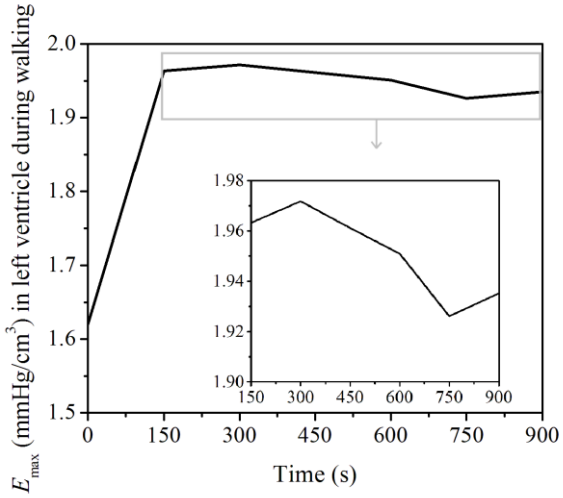


(b)

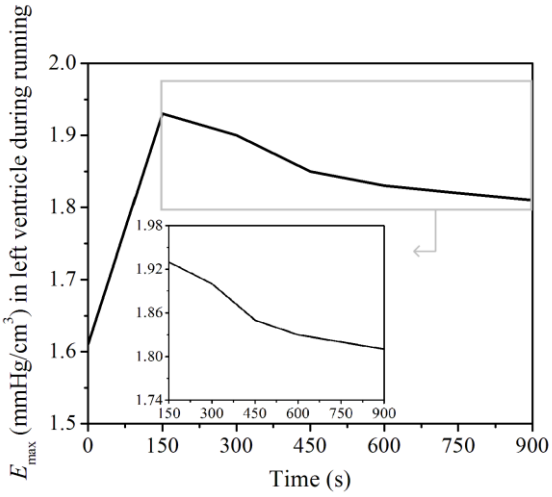


(c)

Fig. 4.9 Maximum elastances in left ventricle during (a) resting, (b) walking and (c) running obtained from BR model

In Fig. 4.10, plots for ESP in left ventricle obtained from BR model are compared for resting, walking and running. These are obtained by considering end systolic volume (ESV) as 50ml. By taking ESV constant, we can directly draw conclusions for ESP for different $E_{max}$ values. During resting, there is not much variation in ESP with the least and most values being 98.82 to 99.88 mmHg. During walking, the ESP varies between 96.31 and 98.59 mmHg. During running, least and most values for ESP at the end and in the starting are 90.50 and 96.50 mmHg, respectively.

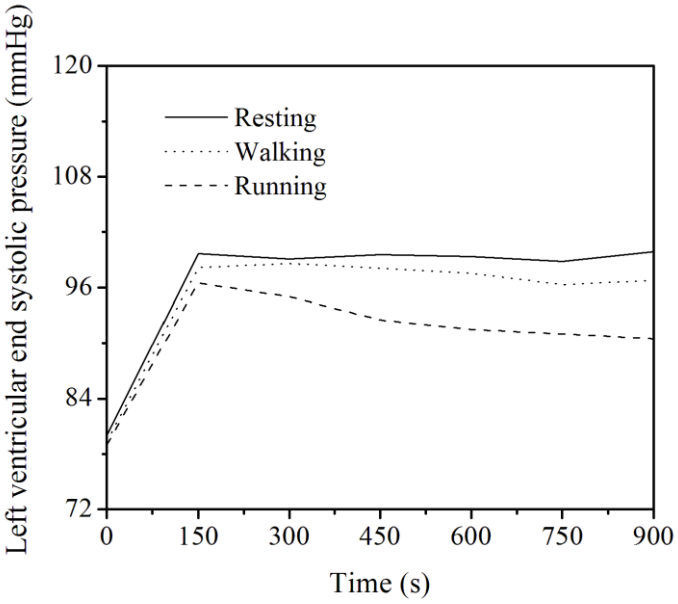


Fig. 4.10 Comparison of approximate left ventricular ESP during resting, walking and running obtained from BR model

• Results from BR model for TMT clinical test

Figure 4.11(a) show systolic and diastolic pressure readings for a patient who underwent clinical TMT. His BP ranges from 128/85 in starting to 160/100 at the end of test. Fig. 4.11(b) shows $E_{max}$ plot for TMT test. Minimum value for $E_{max}$ is 1.770 mmHg/cm$^3$at the end and maximum value is 1.860 mmHg/cm$^3$ in the starting. Figure 4.11(c) shows plot for ESP with least and most values at the end and in the starting are 88.50 and 93 mmHg, respectively.

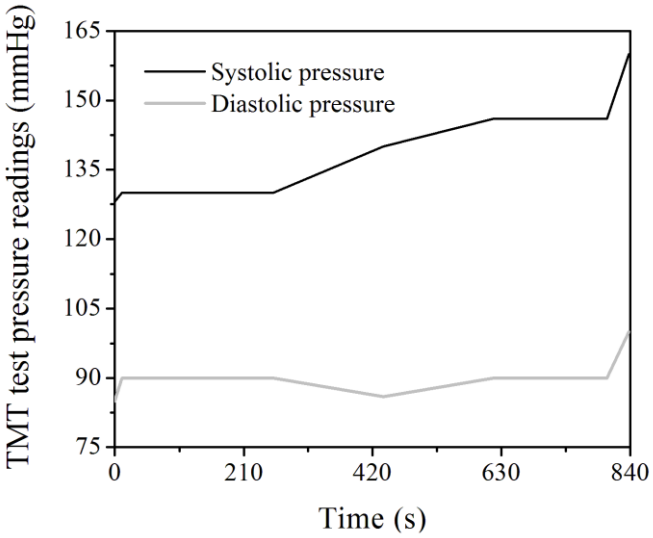


(a)

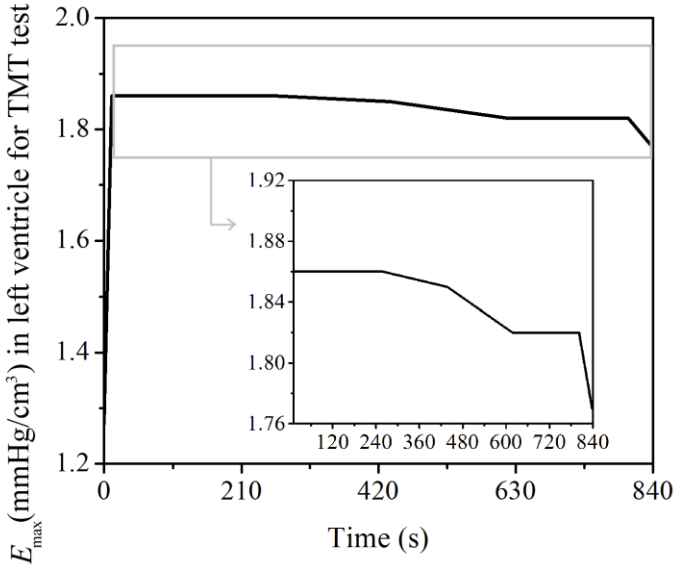


(b)

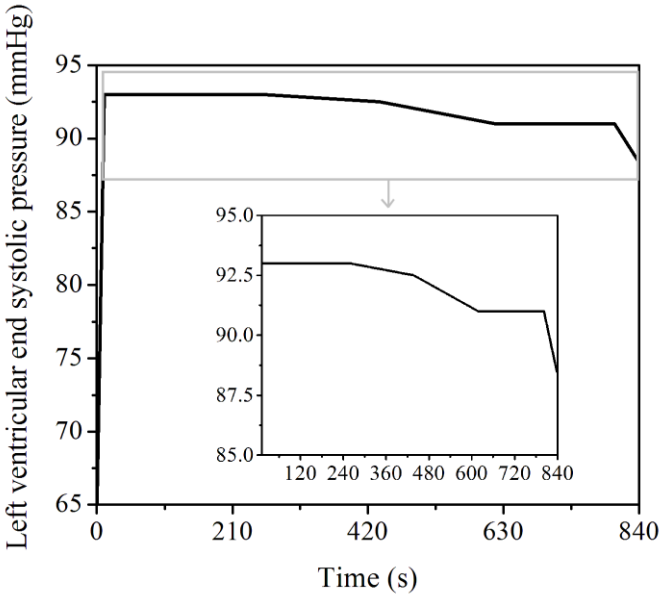


(c)

Fig. 4.11(a) Systolic and diastolic arterial blood pressures measured during clinical TMT test, (b) maximum elastances in left ventricle and (c) approximate ESP for left ventricle during clinical TMT test obtained from BR model

*4.3.2 Parameter values and results for model with overwhelming controller*

- Parameter values for controller are given in Table 4.2.

Table 4.2 Parameter values for controller

| Parameter | Values |
|---|---|
| Controller gain ( $\alpha$ ) | 8.5 |
| Controller resistance ( $R_c$ ) | $1\times10^{7}$ Ns/m$^5$ |
| Controller compliance ( $K_c$ ) | $1\times10^{10}$ N/m$^5$ |
| Controller inertance ( $I_c$ ) | $1\times10^{4}$ Ns$^2$/m$^5$ |

- Results from model with overwhelming controller

Figure 4.12 shows comparison of input and output of an overwhelming controller. TMT test values are given as desired output or input to the system with overwhelming controller. Controller output is fed to the plant which is CVS and output of plant is arterial pressure. In figure, plots with complete lines represent desired output values and the ones with dashed lines represent actual output.

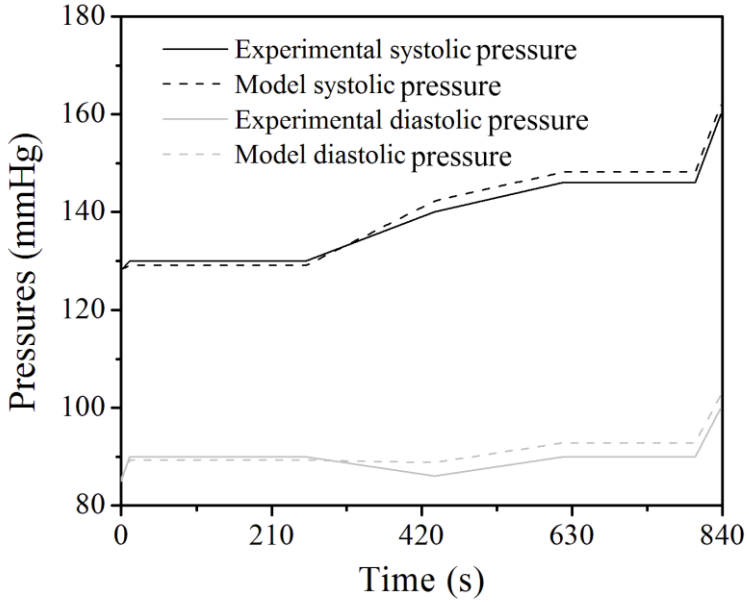


Fig. 4.12 Comparison between arterial blood pressures measured from clinical TMT test and results obtained from overwhelming controller based feedback model

# Chapter 5 Conclusions

## 5.1 Conclusions

The objective of this thesis is to show the applicability of bond graph technique in modelling physiological systems. The system taken into consideration to show the applicability is CVS. Bond graph models for CVS and BR systems were developed and studied. The following conclusions can be drawn from the work done in thesis.

- The simulations of the models developed in this work present good quality results. The results of CVS system are very much similar to the theoretical ones and are in harmony with physiological data and also with work done by others. The very first model discussed in this thesis focussed on generating BP profiles. The inputs taken are clinically suggested ones. The results obtained for blood pressures as output are also comparable to the ones in the real world. So, this shows the reliability of bond graph as a tool in biomedical engineering field.
- A detailed observation of the graphs obtained gives us very minute details about CVS. For example: A notch highlighted in SC, also visible in PC is due to the valve closing at that time.
- Another observation depicts a phase lag in both the circulations. This phase lag is due to viscous elastic properties of the blood vessels.
- These viscous elastic properties of the blood vessels are also responsible for a drop in amplitude of pressure as we move down the vascular tree.
- As noticeable from the comparison that the pressure in the arteries does not fall below a certain limit, but it falls to a very low pressure in ventricles. This can be explained by closing of valves and wave effect as explained in chapter 4.
- The next model applied biological knowledge of BR in developing a model so that the effects of change in BP on left ventricular parameters could be studied. This model shows that for even very fast change in BP, there is an immediate and noticeable change in a very important parameter of the heart. The quick response of bond graph model is highlighted in this work.
- A quick look at the comparisons for all the 3 formats of experiments tells us that there is a good difference between the $E_{max}$ value plots for all of them. This shows that the model reflects actual working of the mechanism.

- The values for $E_{max}$ are lower for higher pressures which means heart muscles are relaxing more than for lower pressures and vice versa.
- The plots for EST also shows a dip in ventricular EST for a rise in BP. This shows that the heart is pumping blood with lower pressure, so that the BP could be brought down.
- The third model for modelling BR mechanism using overwhelming controller in place of ANS also considered in this thesis is very helpful in showing a summed up version of the mechanism and also saved a lot of computational time. Few modifications were made while constructing signal flow graph from bond graph in order to accommodate the modulated resistance in aortic valve region. The error limit between input and output of the system were found to be within acceptable range.

## 5.1 Future scope

Based on the work presented in this thesis, the following work is suggested for future:

- The BR model can be expanded to study the effect of change in BP on other parameters like heart rate, stroke volume and venous resistance *etc*.
- Effects of age and sex on the efficiency of BR to regulate BP can also be added in the model.
- Another plan for future that interests me is to develop a model which can give instantaneous pressure in the heart for every pressure input from arteries. This would be entirely different from what I have done till now as my model only gives the insight into what nervous system should do, but it does not include the actual happenings. So, my model till the work I have done is an ideal model not the actual one.
- The final project I wish to work on is to develop a model which can give diastolic and systolic values for BP. This differs from the work I have done in the sense that my model only gives pressure in the ventricle at a single point of time i.e., at the time of closing of aortic valve. This doesn't give a clear idea of whether the pressure inside the ventricle is within specified limits or not.

# References


[1] Beyar R, Kishon Y, Sideman S and Dinnar U. Computer studies of systemic and regional blood flow mechanisms during cardiopulmonary resuscitation. *Medical and Biological Engineering and Computing* 1984; 22: 499–505.

[2] McInnis B, Guo Z, Chien P and Wang J. Adaptive control of left ventricular bypass assist devices. *IEEE transactions on automatic control* 1985; 30: 322–329.

[3] Mireya D and Marisol D. Modelling and simulation of human cardiovascular system with bond graph: A basic development. *Computers in cardiology* 1996; 23: 393–396.

[4] Sagawa K. The end-systolic pressure-volume relation of the ventricle: definition, modification and clinical use. *American Heart Association* 1981; 63: 1223–1227.

[5] Bera TK, Samantaray AK and Karmakar R. Robust overwhelming control of a hydraulically driven three degrees of freedom parallel manipulator through a simplified fast inverse model. *Journal of Systems and Control Engineering* 2010; 224: 169–184.

[6] Sheila RB, Raymond JM, Dan KK, Margaret G, Gohar A, Knight EL, Jerald CN and Lewis AL. Effects of age and gender on autonomic control of blood pressure dynamics. *Hypertension* 1999; 33: 1195–1200.

[7] Shuzhen C, Shaowen Z, Yuexian G, Kaiyong D, Meirong S, Yi Y and Gangmin N. The role of autonomic nervous system in hypertension: a bond graph model study. *Physiological measurement* 2008; 29: 473–495.

[8] Roon VAM. *Short-term cardiovascular effects of mental tasks*. PhD Thesis, University of Groningen, 1998.

[9] Sagawa K. Representation of cardiac pump with special reference to afterload. In: *Cardiovascular system dynamics, models and measurements*. New York: Plenum Press, 1986, pp. 1–18.

[10] Fung K, Yerin C. Biodynamics. In: *Circulation on Physiology*. New York: Springer-Verlag, 1984.

[11] Klute G, Tasch U and Geselowitz D. An Optimal Controller for an Electric Ventricular Assist Device. *IEEE Transactions on biomedical engineering (Theory, Implementation, and Testing)* 1992; 39: 394–399.

[12] Yoshio I, Jay SM, Katsuhiko T, Jose IG, Chaim Y, Robert WM, Frater R and Edward LY. Left ventricular filling dynamics: influence of left ventricular relaxation and left atrial pressure. *Circulation* 1986; 74: 187-196.

[13] Burkoff D. Mechanical properties of the heart and its interaction with the vascular system. *Cardiac Physiology* 2002; 46:1–23.

[14] Reul H, Minamitani H and Runge J. A hydraulic analog of the systemic and pulmonary circulation for testing artificial hearts. *Journal of European Society for Artificial Organs* 1975; 2: 120–127.

[15] Rolle VL, Hernandez AI, Richard PY, Buisson J and Carrault G. A bond graph model of the cardiovascular system. *Acta Biotheoretica* 2005; 53: 295–312.

[16] Michael RZ, Gerald I, and William HG. Left ventricular diastolic dysfunction limits use of maximum systolic elastance as an index of contractile function. *Circulation* 1991; 83: 674–680.

[17] Xiaoxiao C, Sala XLM, Hammond RL, Masashi I, Soroor SX, Mukkamala R, and Donal SOL. Dynamic control of maximal ventricular elastance via the baroreflex and force-frequency relation in awake dogs before and after pacing-induced heart failure. *American Journal of Physiology-Heart and Circulatory Physiology* 2010; 299: H62–H69.

[18] Stergiopulos NI, Meister JJ and Westerhof NI. Determinants of stroke volume and systolic and diastolic aortic pressure. *American Journal of Physiology-Heart and Circulatory Physiology* 1996; 270: H2050–H2059.

[19] Teddy MC, Andrey VS, Branko GC, Steven WS and Wang L. Nonlinear modelling and control of human heart rate response during exercise with various work load intensities. *IEEE Transactions on biomedical engineering* 2008; 55: 2499–2508.

[20] Gribbin B, Pickering TG, Sleight P and Peto R. Effect of age and high blood pressure on baroreflex sensitivity in man. *Circulation research* 1971; 29: 424–431.

[21] Tanaka M, Kimura T, Goyagi T and Nishikawa T. Gender differences in baroreflex response and heart rate variability in anaesthetized humans. *British Journal of Anaesthesia* 2004; 92: 831–835.

[22] LeFevre J, Tavernier A and Durbaba S. Extended block and bond graphs: A unified formalism for generalised physiological lumped models. *IEEE Proceedings on EMBS (Engineering in medicine and biology society, proceedings of the 15$^{th}$ annual international conference of IEEE*) 1993; 15: 525–526.

[23] Dauphin TG, Sueur C and Rombaut C. Bond-graph approach of commutating phenomena. *Processing in Automatic Control* 1989; 233: 339–343.

[24] Karemaker JM. Neurophysiology of the baroreceptor reflex. *The beat by beat investigation of cardiovascular function* 1987; 102: 27–49.

[25] Scher AM. Cardiovascular control. Textbook of physiology 1989; 2: 972–990.

[26] Berne RM and Levy MN. Cardiovascular physiology 6th ed. St. Louis: Mosby Year Book Inc, 1992.

[27] Guyton AC. Circulatory physiology III: Arterial pressure and hypertension. In: *WB Saunders Company*, Philadelphia, 1980.

[28] Donald DE and Shepherd JT. Autonomic regulation of the peripheral circulation. *Annual review on Physiology* 1980; 42: 429–439.

[29] Hilton SM and Spyer KM. Central nervous regulation of vascular resistance. *Annual review on Physiology* 1980; 42: 399–411.

[30] Chalmers JP. Afferent inputs to ventrolateral medulla. In: *Central neural mechanisms in cardiovascular regulation*, Birkhauser Boston Inc, Boston, 1992; 3–13.

[31] Spyer KM. The central nervous organization of reflex circulatory control. In: *Central regulation of autonomic function*, New York: Oxford University Press, 1989; 168–188.

[32] Giersbergen V, Palkovits M and De JW. Involvement of neurotransmitters in the nucleus tractus solitarii in cardiovascular regulation. *Physiological Review* 1992; 72: 789–824.

[33] Shields RW. Functional anatomy of the autonomic nervous system. *Journal of Clinical Neurophysiology* 1993; 10: 2–13.

[34] Shimizu T and Bishop VS. Mechanism of reflex control of cardiac contractility by carotid sinus baroreceptors. *American Journal of Physiology* 1980; 293: H65–H72.

[35] Brown AM. Receptors under pressure: an update on baroreceptors. *Circulation Research* 1980; 46: 1–10.

[36] Martin PJ, Matthew NL and Zieske H. Bilateral carotid sinus control of ventricular performance in the dog. *Circulation Research* 1969; 24: 321–337.

# Curriculum vitae

Kartik Sharma did his graduation in Mechanical Engineering from North Maharashtra University, Jalgaon in 2012. In 2013 he joined LLOYD INDIA Ltd., Okhla, New delhi in the designing department, where he was given responsibility for designing of air compressors. In 2014, he joined Masters of Engineering Programme Thapar University, Patiala in CAD/CAM Engineering, through GATE 2013. His ME thesis was in the area of biomedical engineering and his specific stream was cardiovascular engineering. One paper from his work ‘A Bond Graph Approach to the Modelling of Cardiovascular System with Embedded Autonomic Nervous System’ has been communicated into the journal “Acta Biotheoretica”, Springer publisher. Another journal paper is under preparation.